Società Geologica Italiana

ISPRA
Istituto Superiore per la Protezione e la Ricerca Ambientale
SERVIZIO GEOLOGICO D'ITALIA
Organo Cartografico dello Stato (legge N°68 del 2-2-1960)
Dipartimento Difesa del Suolo

Geological Field Trips

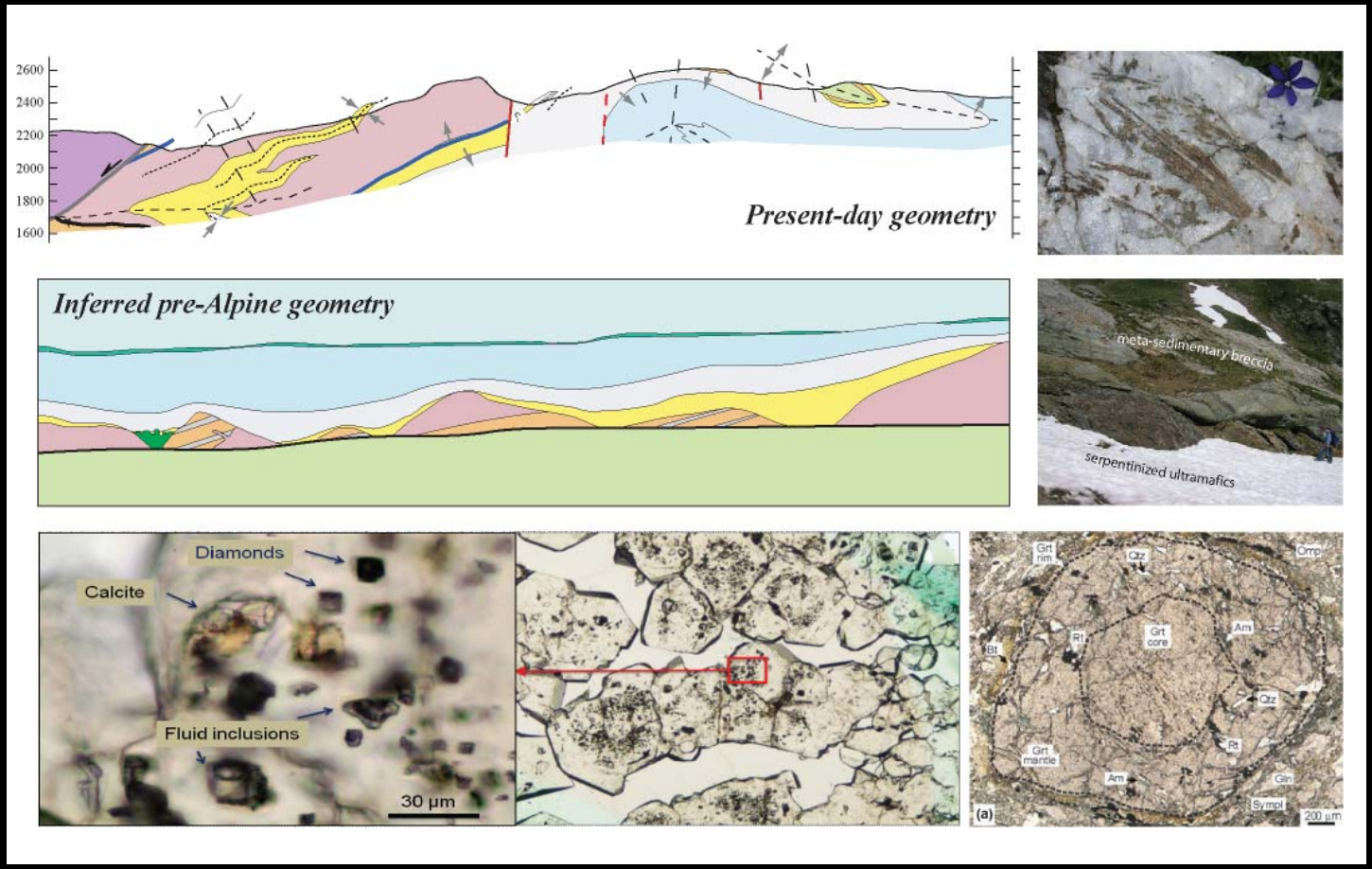

2014
Vol. 6 (1.1)

ISSN: 2038-4947

From passive margins to orogens: the link between Zones of Exhumed Subcontinental Mantle and (U)HP metamorphism

10th International Eclogite Conference - Courmayeur (Aosta, Italy), 2013

DOI: 10.3301/GFT.2014.01

GFT - Geological Field Trips

Periodico semestrale del Servizio Geologico d'Italia - ISPRA e della Società Geologica Italiana
Geol.F.Trips, Vol.**6** No.1.1 (2014), 61 pp., 26 figs. (DOI 10.3301/GFT.2014.01)

From passive margins to orogens: the link between Zones of Exhumed Subcontinental Mantle and (U)HP metamorphism

10th International Eclogite Conference, Courmayeur (Aosta, Italy) - Pre-conference excursions: September 2-3, 2013

Marco BELTRANDO[1], Roberto COMPAGNONI[1], Jaime BARNES[2], Maria Luce FREZZOTTI[3], Daniele REGIS[4], Gianluca FRASCA[5], Marnie FORSTER[6], Gordon LISTER[6]

[1] Department of Earth Sciences, University of Torino, via Valperga Caluso 35, 10125 Turin, Italy
[2] Department of Geological Sciences, Jackson School of Geosciences, University of Texas at Austin, 2275 Speedway Stop C9000, Austin, Texas 78712 (USA)
[3] Department of Earth and Environmental Sciences, University of Milano Bicocca, P.zza della Scienza 4, 20126 Milan, Italy
[4] Department of Environment, Earth and Ecosystems, The Open University, Walton Hall, Milton Keynes MK7 6AA, United Kingdom
[5] Géosciences Rennes, UMR 6118, Université de Rennes 1, Campus de Beaulieu, 35042 Rennes Cedex, France
[6] Research School of Earth Sciences, Mills Rd, Australian National University, Canberra, ACT 0200, Australia

Corresponding Author e-mail address: marco.beltrando@unito.it

ISSN: 2038-4947 [online]

http://www.isprambiente.gov.it/it/pubblicazioni/periodici-tecnici/geological-field-trips

DOI: 10.3301/GFT.2014.01

INDEX

Information

Excursion notes

Itinerary

DOI: 10.3301/GFT.2014.01

DOI: 10.3301/GFT.2014.01

Information

Day 1

Altitude: 2100-2550 m a.s.l.
Elevation gain (on foot): ca. 150 m along an easy path, followed by ca. 300 m on grassy slopes

Day 2

Altitude: ca. 2150 m a.s.l.
Elevation gain (on foot): none

Safety

Mountain boots, sun glasses and sunscreen are strongly recommended. Considering that sudden weather changes are likely to happen in Alpine settings, water and windproof clothes are also recommended.

Hospital

Aosta
Ospedale Regionale
Viale Ginevra 3, Aosta,
Tel. +39 0165 5431 ý
0165 5431

Accomodation

Hotel Pavillon
Strada Regionale 62, 11013 Courmayeur
Tel: +39 0165 846120

Location of the two excursion days

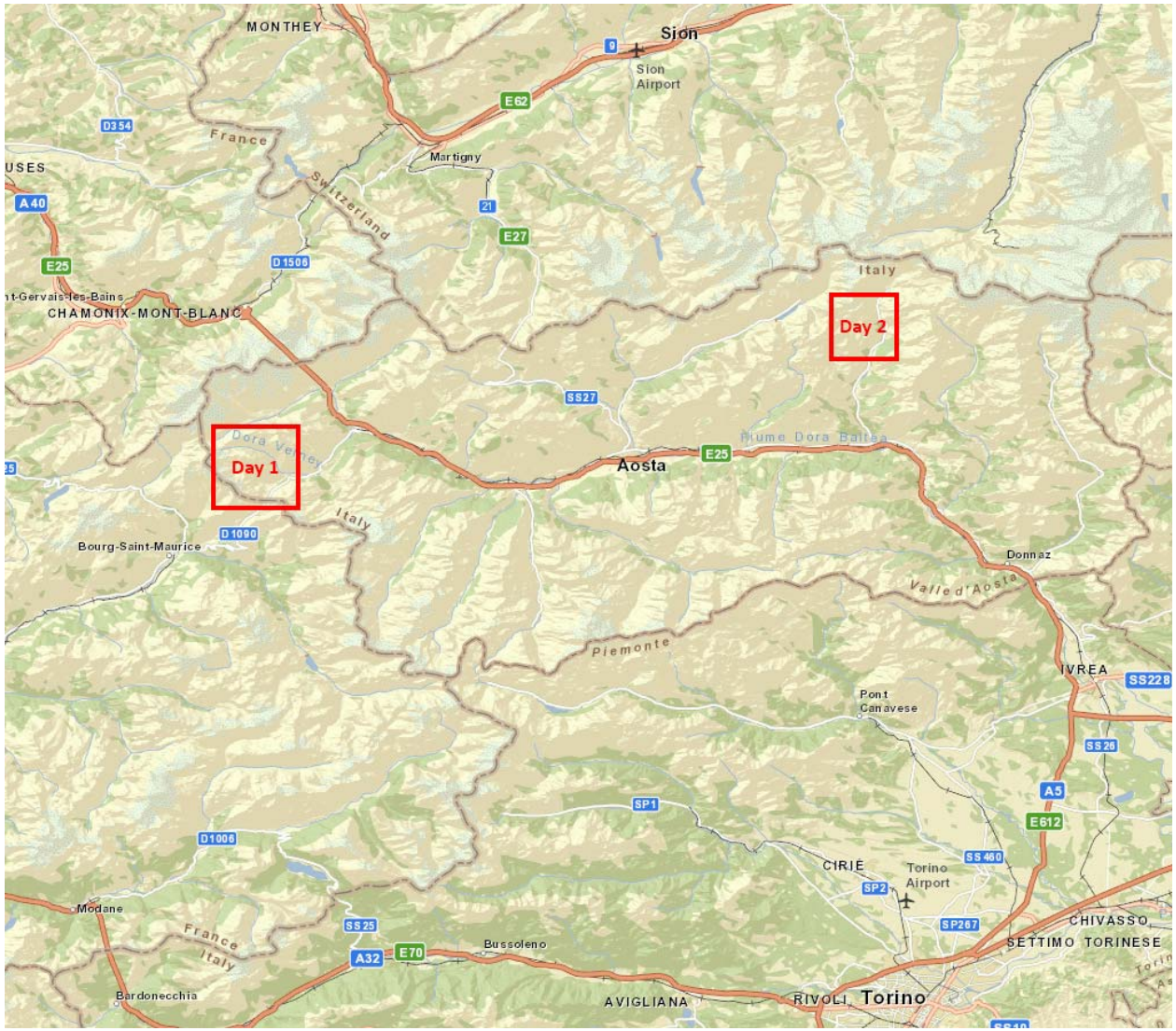

DOI: 10.3301/GFT.2014.01

Localization of the route of the first day

Localization of the route of the second day

DOI: 10.3301/GFT.2014.01

Riassunto

In questa escursione verranno trattati alcuni temi connessi all'evoluzione della crosta ofiolitica delle Alpi Occidentali dal rifting Giurassico al successivo metamorfismo di (ultra-)alta pressione nell'Eocene-Oligocene. Le tematiche principali verteranno (1) sull'architettura delle unità di (U)HP, (2) sull'evoluzione deformativa polifasica durante la subduzione/esumazione e (3) sul significato geodinamico circa la presenza di scaglie di basamento continentale giustapposte a peridotiti serpentinizzate ed a sedimenti di sin- e post-rift, comune a molte unità ofiolitiche alpine di alta pressione. Nel corso della prima giornata, al Passo del Piccolo San Bernardo, osserveremo le relazioni tra basamento continentale Paleozoico, mantello sotto-continentale serpentinizzato e sedimenti di sin- e post-rift, stabilitesi prima dell'orogenesi alpina. Tali relazioni sono preservate nonostante un'evoluzione deformativa polifasica accompagnata da metamorfismo a P≥1.5GPa. Relazioni analoghe tra questi litotipi sono tipiche delle "Zones of Exhumed Subcontinental Mantle" (ZESM) presenti lungo i margini attuali poveri in magma. In tali contesti il mantello sotto continentale viene esumato per l'attività di sistemi di faglie a basso angolo e grande rigetto. Tale tettonica estensionale può portare al campionamento di sezioni di basamento continentale di tetto, dando così origine ai cosidetti 'alloctoni estensionali'. I ritrovamenti effettuati in alcune unità alpine ad ofioliti, quindi, indicano che associazioni litostratigrafiche che consistono di mantello sotto-continentale serpentinizzato, basamento continentale e sedimenti di sin- e post-rift non sono necessariamente legate a dinamiche subduttive complesse, ma possono altresì essere ereditate dalle fasi estensionali pre-subduzione. Nel corso della seconda giornata tratteremo l'evoluzione tettono-metamorfica di sedimenti di post-rift, basalti di fondo oceanico nell'unità di (ultra-)alta pressione del Lago di Cignana, con particolare attenzione ai recenti ritrovamenti di micro-diamanti inclusi nei granati di noduli in quarziti manganesifere. In quest'area la deformazione polifasica durante gli stadi esumativi è stata accomodata da varie generazioni di zone di taglio, accompagnate dalla formazione di pieghe. Per questa ragione non è stato fino ad ora possibile riconoscere sezioni coerenti di crosta giurassica analoghe a quella mostrata nel corso del primo giorno di questa escursione.

Parole chiave: Alpi Occidentali, margini di rift poveri in magma, eclogite, eredità strutturale, quarziti a granatiti manganesifere, diamante.

DOI: 10.3301/GFT.2014.01

Abstract

This excursion deals with the evolution of the ophiolite-bearing crust of the Western Alps from Jurassic rifting to Eocene-Oligocene (ultra-)high-pressure metamorphism. The main topics of this excursion are: (1) the architecture of (U)HP units; (2) multi-stage deformation during subduction/exhumation; (3) the geodynamic significance of continental basement juxtaposition with serpentinized peridotites and syn- to post-rift sediments, which is common to several alpine (U)HP ophiolites.
During the first day, at the Petit St. Bernard pass, we will show that continental basement, serpentinized sub-continental mantle and metasediments preserve pre-Alpine rift-related relationships, despite having undergone multiple phases of alpine deformation and metamorphism at $P \geq 1.5$GPa. Similar relationships are typical of Zones of Exhumed Subcontinental Mantle (ZESM), observed along present-day magma-poor rifted margins, where sub-continental mantle is exhumed at the basin floor through the activity of low-angle detachment faults. Fault activity may locally result in sampling of hangingwall material, including continental basement, which then resides on the fault plane as an "extensional allochthon". These findings indicate that the presence of serpentinized ultramafics alongside continental basement and syn- to post-rift sediments, which is common to several alpine metamorphic terrains, is not necessarily related to complex subduction dynamics, but it may also be inherited from the pre-subduction history.
During the second day, a visit to the Lago di Cignana ultra-high pressure unit will give us the opportunity to discuss the tectono-metamorphic evolution of early-post rift metasediments and metabasalts in the light of the recent finding of microdiamond inclusions in garnet from Mn-bearing quartzites. Multi-stage exhumation-related shuffling of the tectono-metamorphic pile, together with late-stage folding, prevents the recognition of coherent sections of Jurassic crust of the kind observed during the first day.

Keywords: Western Alps, magma-poor rifted margin, eclogite, structural inheritance, quartzite with manganesiferous garnetite, diamond.

DOI: 10.3301/GFT.2014.01

Program summary

The Punta Rossa unit, which will be visited on the **first day**, crops out in the Breuil Valley, near the Petit St. Bernard Pass, at the French-Italian border (Fig. 1). The pass will be approached from La Thuile, in Italy. The western side of the Breuil Valley, which is the target of this excursion, can be reached following track number 14, which starts at the parking area near Lac de Verney, close to the National Route 26. To reach this parking area, driving up from La Thuile, leave the main road at a sharp left bend at the altitude of 2110 m, when you are already in sight of the pass and drive for 50 meters on an unsealed road heading right. Due to the relatively high altitude of the area, in the 2100-2550 m range, this fieldtrip can only be

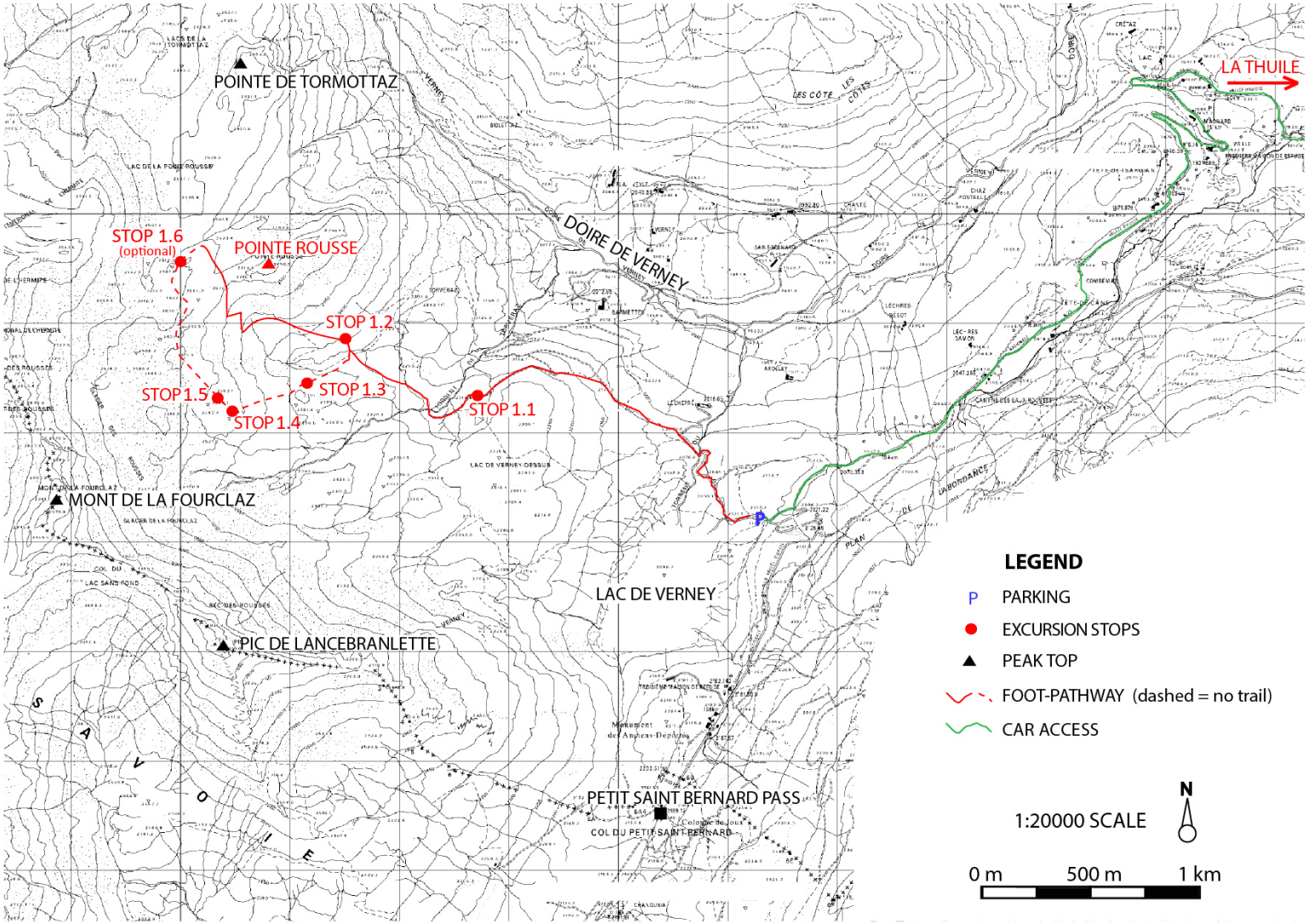

Fig. 1 - Topographic map of the Petit St. Bernard Pass area with access route and excursion Stops.

DOI: 10.3301/GFT.2014.01

undertaken during the summer. Please, note that many outcrops can still be covered in snow in June. August to early September is normally the best time of the year to avoid any snow cover. Several outcrops described in this field guide are located away from the main track and can be accessed only by walking on moderately steep grassy and rocky slopes. Therefore, adequate hiking gear is recommended, as well as warm and water proof clothes, as this area is often windy and weather changes can occur rapidly. Mobile phone coverage in the Breuil valley is generally good. Also note that the area is devoid of suitable shelters in case of unexpected storms.

To reach Lago di Cignana on the **second day**, drive to Antey Saint André, in Valtournenche, then take the road to Torgnon up to the locality Champtornè-Dès (1885 m a.s.l.). Only minivans and cars can continue from here along an unsealed road up to the Lago di Cignana dam (Fig. 2). Please note that a permit must be requested to the Torgnon municipality to drive on this road. This drive is about 15 km long. All excursion stops are located in close vicinity to the road.

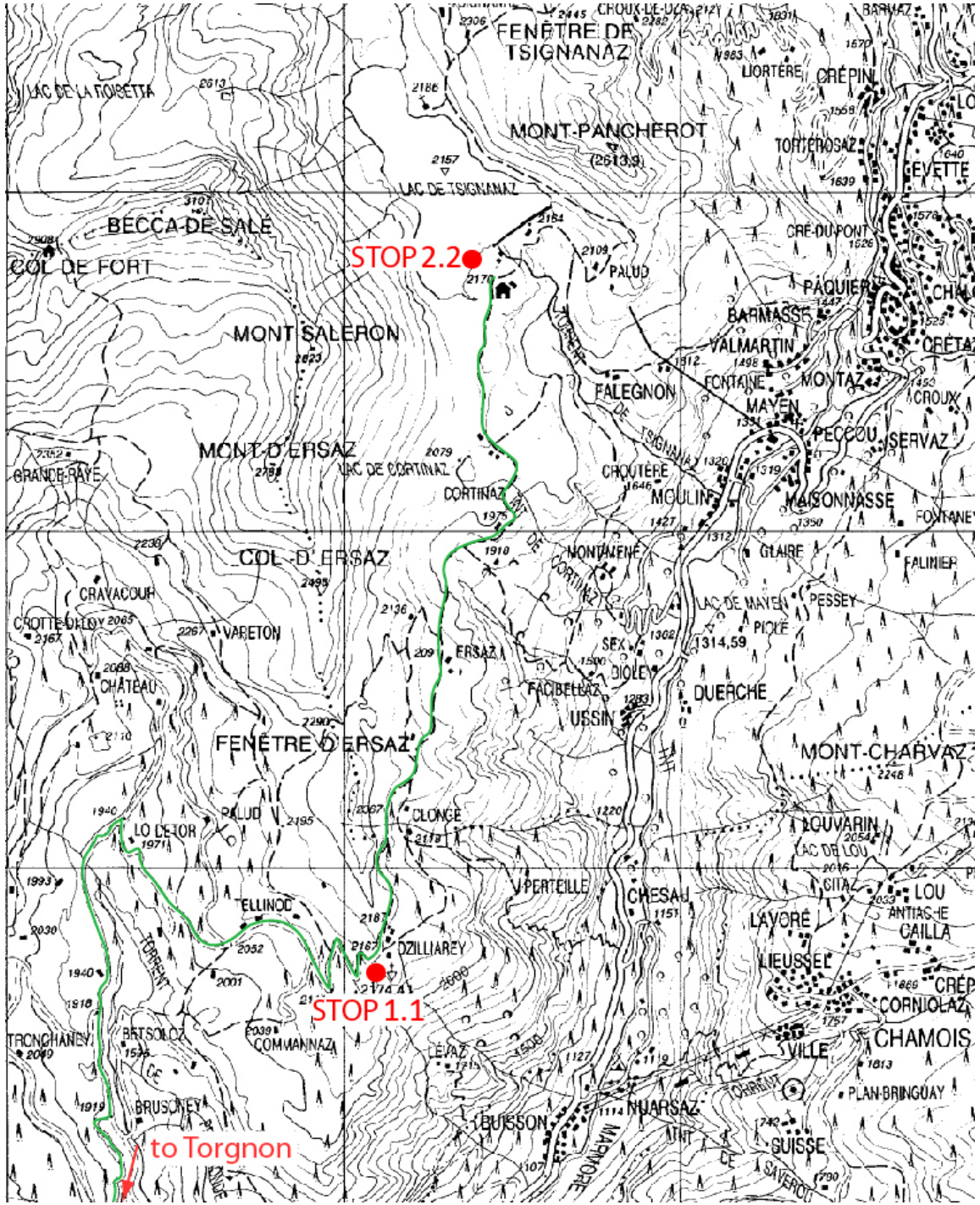

Fig. 2 - Topographic map of the Lago di Cignana area with access route and excursion Stops.

DOI: 10.3301/GFT.2014.01

1. Excursion aims

Orogenic belts, sampling fossil subduction zones, provide key natural laboratories to investigate convergent margin dynamics (e.g. Agard et al., 2009; Beltrando et al., 2010a). In this context, elucidating the pre-orogenic lithostratigraphy of the tectono-metamorphic units stacked in the mountain belt has important implications for understanding the processes leading to their sampling from the downgoing plate and their subsequent exhumation.

In the high-pressure part of Alpine-type orogenic belts, ophiolite-bearing units often consist of Paleozoic continental basement slivers cropping out alongside Jurassic ophiolites and syn- to post-rift sediments (e.g. Dal Piaz, 1999; Beltrando et al., 2010b and 2012; Meresse et al., 2012; Vitale Brovarone et al., 2011). These seemingly 'anomalous' lithological associations are commonly ascribed to complex orogen dynamics, including centrifuge-like flow in a subduction channel (e.g. Polino et al., 1990; Gerya et al., 2002). However, studies conducted over the past 30 years both in present-day rifted margins (e.g. Peron Pinvidic & Manatschal, 2009) and in fossil analogues preserved in the weakly deformed Eastern Alps (Froitzheim & Manatschal, 1996; Manatschal, 2004; Manatschal et al., 2006) provided compelling evidence of the existence of a specific type of transitional lithosphere between typical 'oceanic' and 'continental' lithosphere. These transitional domains, which can be up to 200 km wide, comprise the distal continental margin and the so-called "Zone of Exhumed Subcontinental Mantle" (ZESM). In the distal continental margin, thinned continental crust (<10 km) is directly onlapped by post-rift sediments. As continental crust thins out oceanward, this area grades into the ZESM, where subcontinental mantle is exhumed at the seafloor by the activity of long-offset detachment faults. As a result of the activity of detachment systems, serpentinized mantle can be overlain by slivers of continental crust derived from the stretched hangingwall. The resulting basement topography exerts a strong control on the distribution of syn-rift sediments, which are then sealed by typical pelagic post-rift sediments. Typical distal continental margins and ZESM's have already been extensively recognized in sections of peri-Mediterranean mountain belts that were only marginally affected by orogeny-related deformation/metamorphism (e.g. Decandia & Elter, 1972; Froitzheim & Eberli, 1990; Florineth & Froitzheim, 1994; Molli, 1996; Durand-Delga et al., 1997; Marroni et al., 1998; Manatschal, 2004; Mohn et al., 2012; Beltrando et al., 2013). More recently, lithological associations with slivers of continental basement resting upon serpentinized ultramafics in the high-pressure to ultra-high-pressure Piemonte units of the Western Alps and Corsica have been interpreted as

DOI: 10.3301/GFT.2014.01

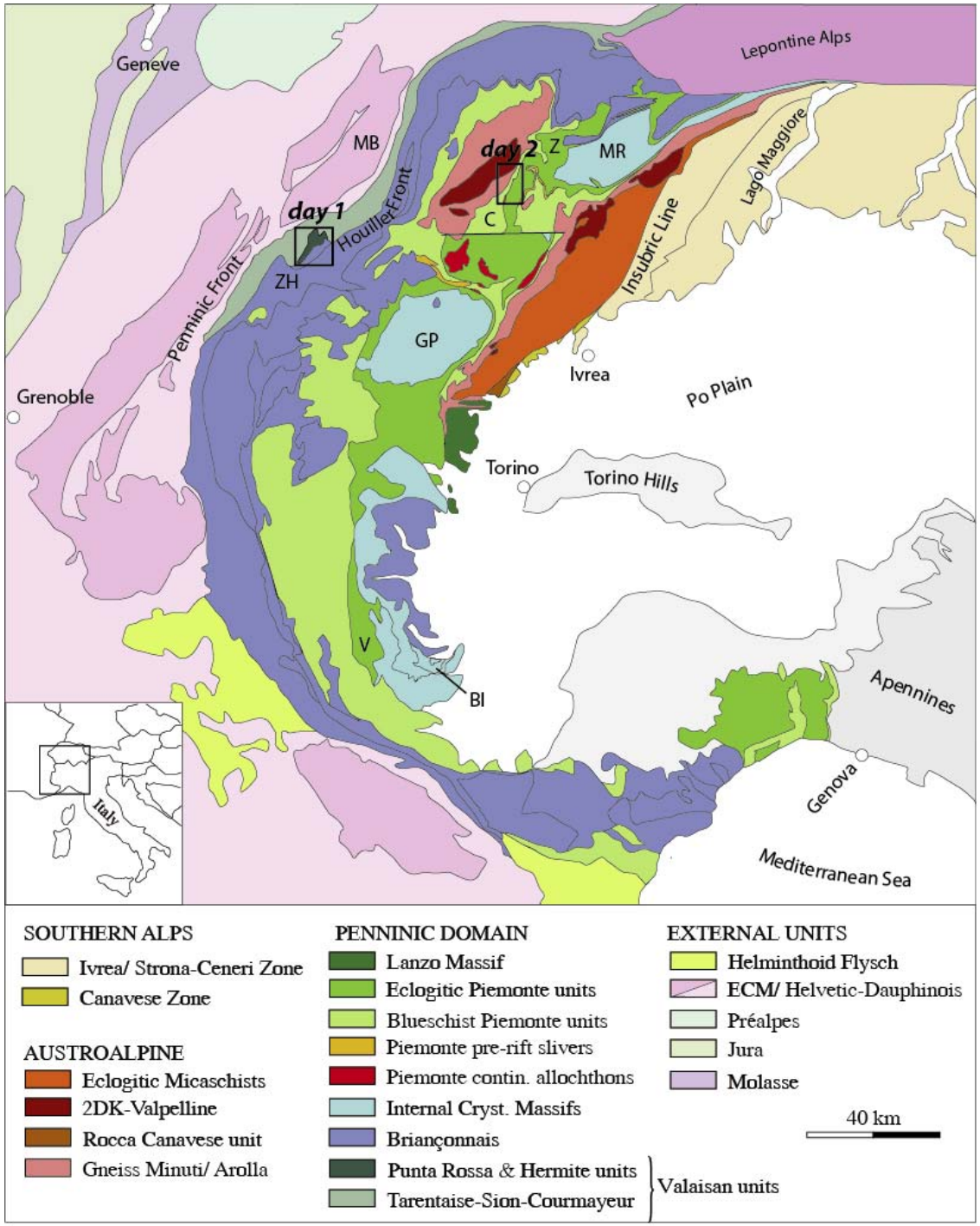

remnants of Jurassic ZESM's (Dal Piaz, 1999; Beltrando et al., 2010b; Vitale Brovarone et al., 2011; Meresse et al., 2012). Similar findings in the Valaisan domain of the Western Alps (Loprieno et al., 2011; Beltrando et al., 2012) suggest that ZESM's may be much more common than hitherto recognized.

During excursion days (Fig. 3) we will first visit the best-preserved example of a Mesozoic ZESM sampled within the Western Alps, at the Petit St. Bernard Pass. In this locality, a combination of structural, petrologic and lithostratigraphic observations indicates that the different rock types were already juxtaposed prior to the Alpine orogeny. In the Lago di Cignana area, instead, Alpine deformation largely erased pre-orogenic relationships among the different rocks types. However, several lines of evidence indicate that this (U)HP unit was originally part of a "Zone of Exhumed Subcontinental Mantle", too.

Fig. 3 – Simplified tectonic map of the Western Alps (from Beltrando et al., 2010). BI: UHP Brossasco-Isasca unit; C: Combin unit; GP: Gran Paradiso Massif; MB: Mont Blanc Massif; MR: Monte Rosa Massif; V: Monviso; Z: Zermatt-Saas unit; ZH: Houiller Zone. The areas that will be visited during excursion days are indicated.

DOI: 10.3301/GFT.2014.01

2. Jurassic paleogeography of the Alpine Tethys

Since the early '80's, a large number of studies has been devoted to constraining the pre-orogenic paleogeography of the area that was later involved into the Alpine orogeny in the Western Mediterranean (see Mohn et al., 2010, Masini et al., 2013 and references therein). The generally accepted view of the paleogeography of this domain consists of two continental masses, namely the Adriatic/African plate and the European plate, separated by an oceanic basin, labeled Western Tethys (Fig. 4). This basin was characterized by a main branch, known as South Penninic (or Piemonte-Liguria) basin, and a minor northerly branch, the North Penninic (or Valaisan) basin (e.g. Trümpy, 1980; Lemoine, 1985). The two sub-basins, in the area that later became part of the Western and Central Alps, were separated by a continental high, the Briançonnais rise (e.g. Trümpy, 1949; Lemoine, 1985). Several paleogeographic reconstructions suggest that the Western Tethyan basin was highly fragmented by regional-scale EW-trending transform faults (e.g. Lemoine, 1985). Subsequent studies performed in little deformed parts of the Alpine belt have progressively refined this early picture (Fig. 4), showing that large areas of the Piemonte-Liguria and Valaisan basins were floored by partly serpentinized sub-continental mantle (e.g. Manatschal & Müntener, 2008) and that thinned continental basement directly overlain by syn- to post-rift sediments marked the transition from the proximal Adriatic margin to the Piemonte-Liguria basin (Froitzheim & Eberli, 1990; Masini et al., 2011). The resulting paleogeography, chiefly based on observations performed in the little deformed Eastern Alps, consists of an Adriatic proximal margin, preserved in the upper Austroalpine nappes, grading outboard into a necking zone, preserved in the middle Austroalpine nappes (Mohn et al., 2012) then followed by the distal continental margins, floored by exhumed crust, now sampled in the lower Austroalpine nappes. The areas floored by exhumed mantle belonging to the South Penninic basin are now best preserved in the Forno, Platta and Totalp units.

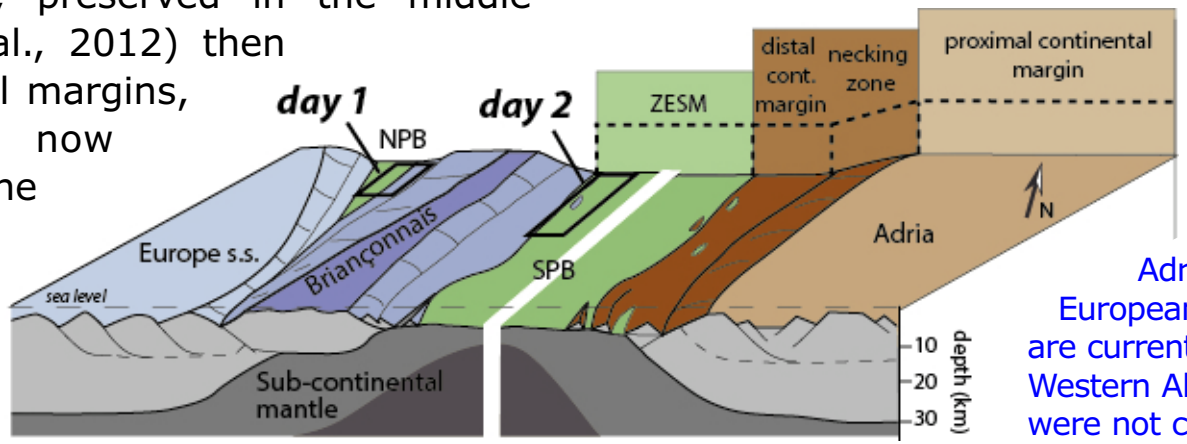

Fig. 4 – Western Tethys paleogeography (modified after Mohn et al., 2010). Note that the Adriatic and European margins, which are currently stacked in the Western Alps, originally were not conjugate.

DOI: 10.3301/GFT.2014.01

DAY 1

3. Punta Rossa unit (Valaisan domain): Mesozoic rift-related juxtaposition of sub-continental mantle, continental basement and sediments and their interaction during Alpine metamorphism

3.1 Introduction

The Valaisan domain, near the Petit St. Bernard Pass, consists of serpentinized sub-continental mantle juxtaposed to Paleozoic basement, Mesozoic pillow meta-basalts and Mesozoic to Tertiary meta-sediments, which underwent Alpine metamorphism at $P \geq 1.5$ GPa (Cannic et al., 1996; Bousquet et al., 2002). A recent structural, lithostratigraphic and metamorphic study (Beltrando et al., 2012) showed that this complex lithostratigraphic association was largely established during rift-related extensional tectonics and underwent relatively minor reworking during the Alpine orogeny. Mantle peridotites were exhumed at the bottom of the North Penninic basin by extensional faulting, resulting in widespread cataclasis of continental basement rocks, which rested above serpentinized mantle as extensional allochthons. The serpentinite-Paleozoic basement pair was sealed by locally-sourced polymictic breccias, prior to the deposition of radiolarian-bearing gray micaschists, followed by other basinal metasediments, including calcschists. Despite subsequent Alpine deformation and metamorphism, resulting in multi-stage folding and medium *P*-low *T* metamorphism, the rift-related relationships among the different rock types can still be observed or inferred in several localities. This field guide presents a one day excursion aimed at illustrating some of the key features that allow reconstructing the pre-Alpine lithostratigraphy, alongside a few stops where the present-day architecture of this domain is described. The description of the serpentinites is also enriched by geochemical data, which will be presented during the excursion, documenting the origin of these mantle peridotites as well as the multiphase hydration during subduction and metamorphism, through interaction with sediment-derived fluids.

3.2 Geological setting

The Valaisan domain, in the Western Alps, is bounded towards the NW by the Penninic Front, which separates the Valaisan units from the more external Helvetic-Dauphinois domain (Fig. 3). The latter consists of Paleozoic basement overlain by a Late Permian to Lower Oligocene sedimentary cover sequence, typical of the European

DOI: 10.3301/GFT.2014.01

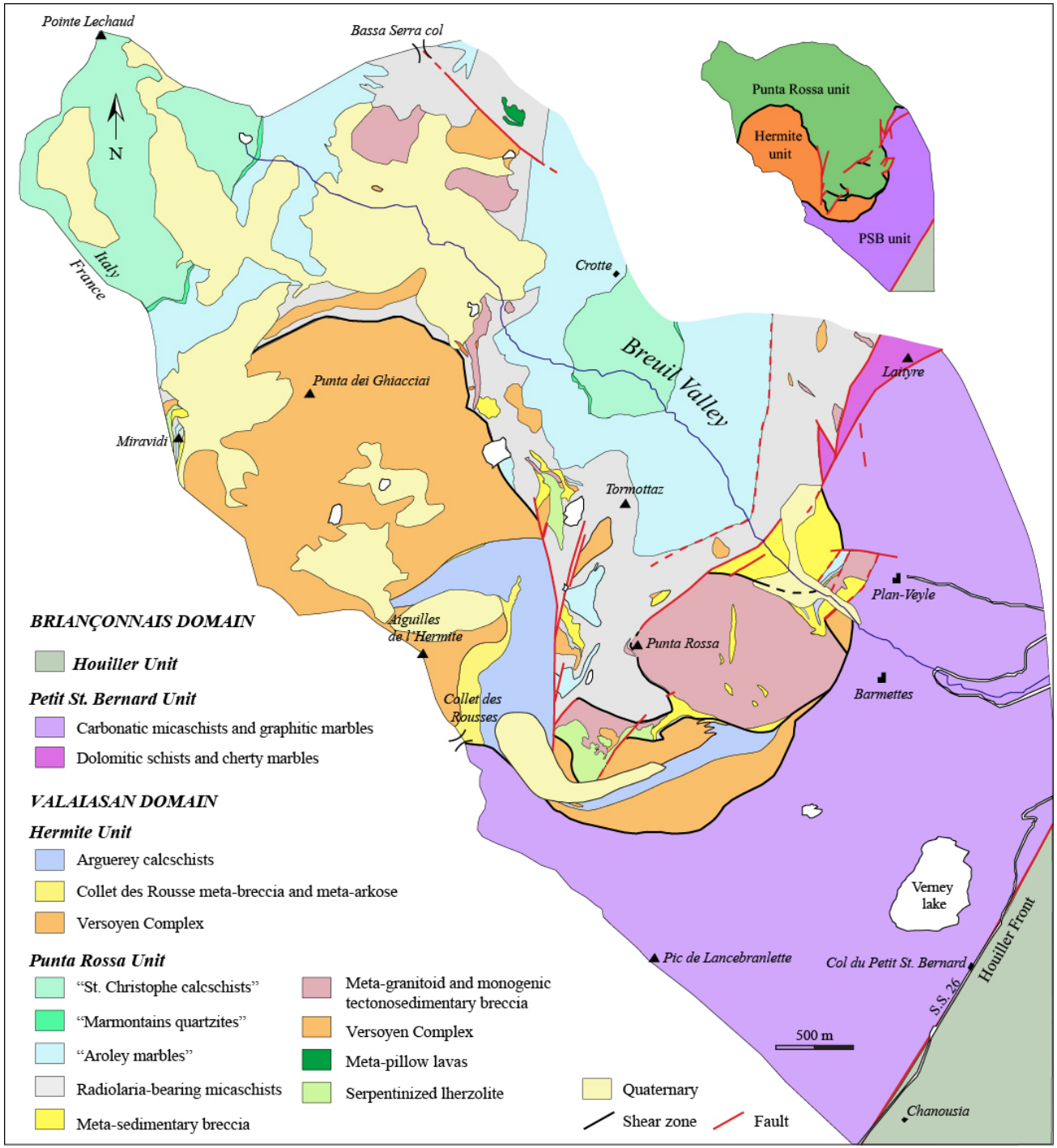

proximal rifted margin (Escher et al., 1997). Towards the SE, instead, the Houiller Front separates the Valaisan units from the overlying Houiller Zone (Fig. 3 and 5). The latter belongs to the Briançonnais domain, which consists of tectonic units originated from a continental rise separating the North and South Penninic basins. The Houiller Zone consists of Carboniferous and Permian sandstone, breccia and shale of continental origin, with minor Early Triassic dolomite and shale, which underwent relatively minor Alpine metamorphism at P= 0.6 ± 0.2 GPa and T= 280-300°C (Lanari et al., 2012).

Fig. 5 – Simplified geological map of the Valaisan units in the Breuil Valley. Inset shows the different tectono-stratigraphic units detected in the area (from Beltrando et al., 2012).

DOI: 10.3301/GFT.2014.01

The Valaisan units, in the Petit St. Bernard pass area, at the French-Italian border, have been the subject of several recent studies (Cannic et al., 1995 and 1996; Fügenschuh et al., 1999; Schärer et al., 2000; Bousquet at al., 2002; Beltrando et al., 2007; Masson et al., 2008; Mugnier et al., 2008; Loprieno et al., 2011; Beltrando et al., 2012 and references therein). The pre-Alpine lithostratigraphy of the Valaisan domain between the Penninic front and the Petit St. Bernard pass indicates an original paleogeographic position along the European escarpment, between the European plate *sensu stricto* and the Briançonnais rise (Fig. 4; Loprieno et al., 2011). Evidence of mantle exhumation at the seafloor indicates that complete crustal excision was achieved, at least locally, within this basin (Loprieno et al., 2011; Beltrando et al., 2012). The Valaisan domain, in the Petit St. Bernard area, can be subdivided into the Hermite and Punta Rossa sub-units (Figs. 5, 6 and 7), which are separated by a late-stage shear zone (Stop 1.2) (Beltrando et al., 2012). Despite this subdivision, the two units display a similar tectono-metamorphic evolution and lithostratigraphy. However, serpentinites are exclusively found in the Punta Rossa unit, which is the main focus of this excursion.

In the Petit St. Bernard pass area, the small Petit St. Bernard unit crops out between the Houiller zone and the Valaisan domain (Fig. 5). The Petit St. Bernard unit consists of marbles and dolostones, originated from upper Triassic dolomitic schists and Lower Jurassic cherty marbles, overlain by calcschists (Elter & Elter, 1957). The calcschists consist of belemnite-bearing carbonate micaschists and graphitic marbles (Franchi, 1899), interpreted as Early to Middle Jurassic in age (Elter & Elter, 1965). This unit has generally been considered as an independent Alpine tectono-metamorphic unit, separated from the mafic/ultramafic bearing units underneath by Alpine shear zones (e.g. Elter & Elter, 1957, Antoine et al., 1992; Bousquet et al., 2002, Beltrando et al., 2012; see Masson et al., 2008 and Loprieno et al., 2011 for alternative interpretations). This view is supported by the distinctive lithostratigraphy and by its tectono-metamorphic evolution (Beltrando et al., 2012), including the estimated timing of Alpine metamorphism, in the 43-45 Ma range (^{40}Ar-^{39}Ar step heating on white mica; Cannic, 1996).

3.3 Lithostratigraphy of the Punta Rossa unit

The Punta Rossa unit consists of serpentinized subcontinental mantle, Paleozoic basement, rare Mesozoic pillowed meta-basalts and different types of Mesozoic metasediments. Only the general features of the different rock types are recalled here, as a more detailed discussion is presented in the excursion stops.

DOI: 10.3301/GFT.2014.01

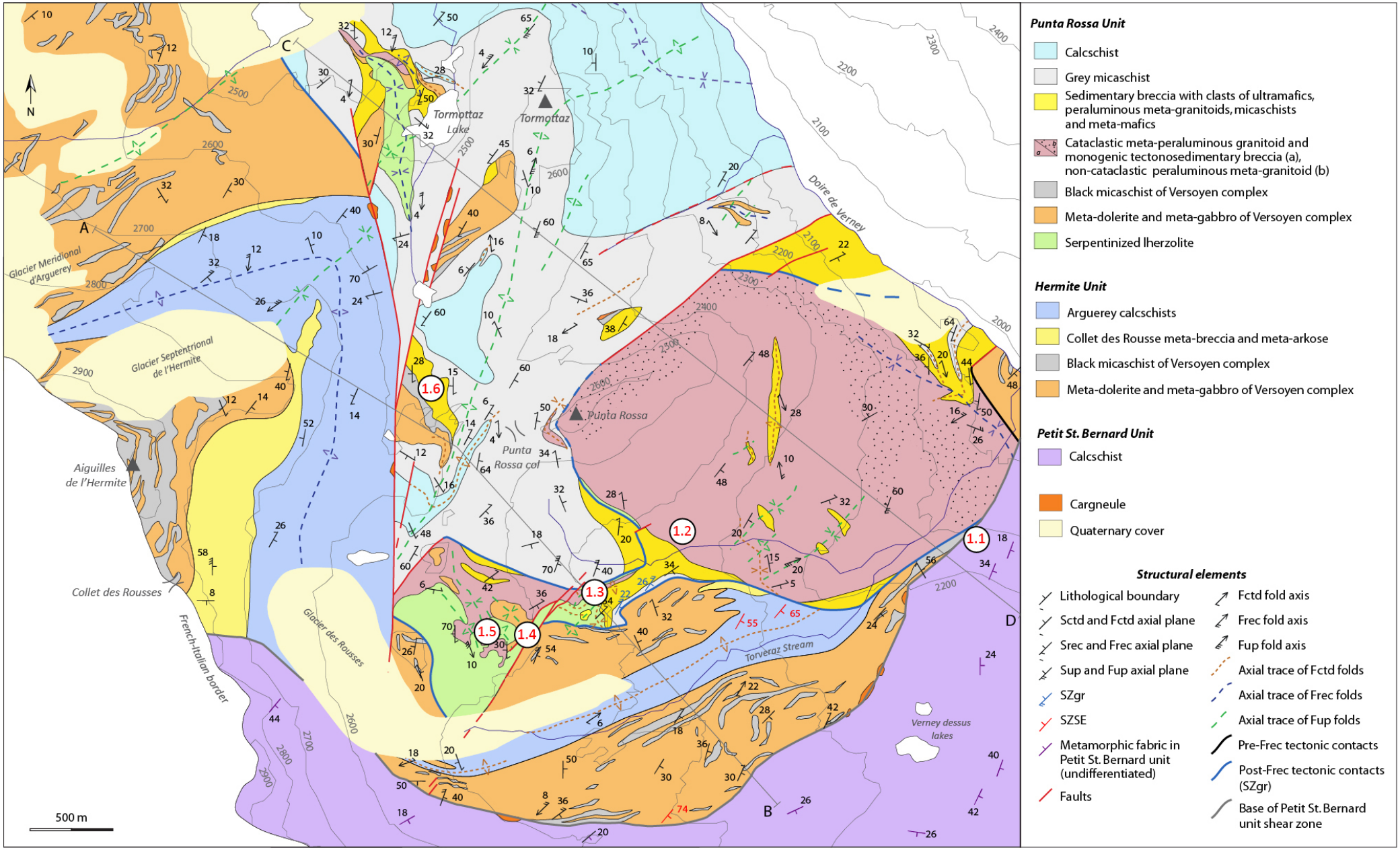

Fig. 6 - Geological map with excursion stops (from Beltrando et al., 2012). Traces of geological cross sections shown in Figure 7 are also indicated.

DOI: 10.3301/GFT.2014.01

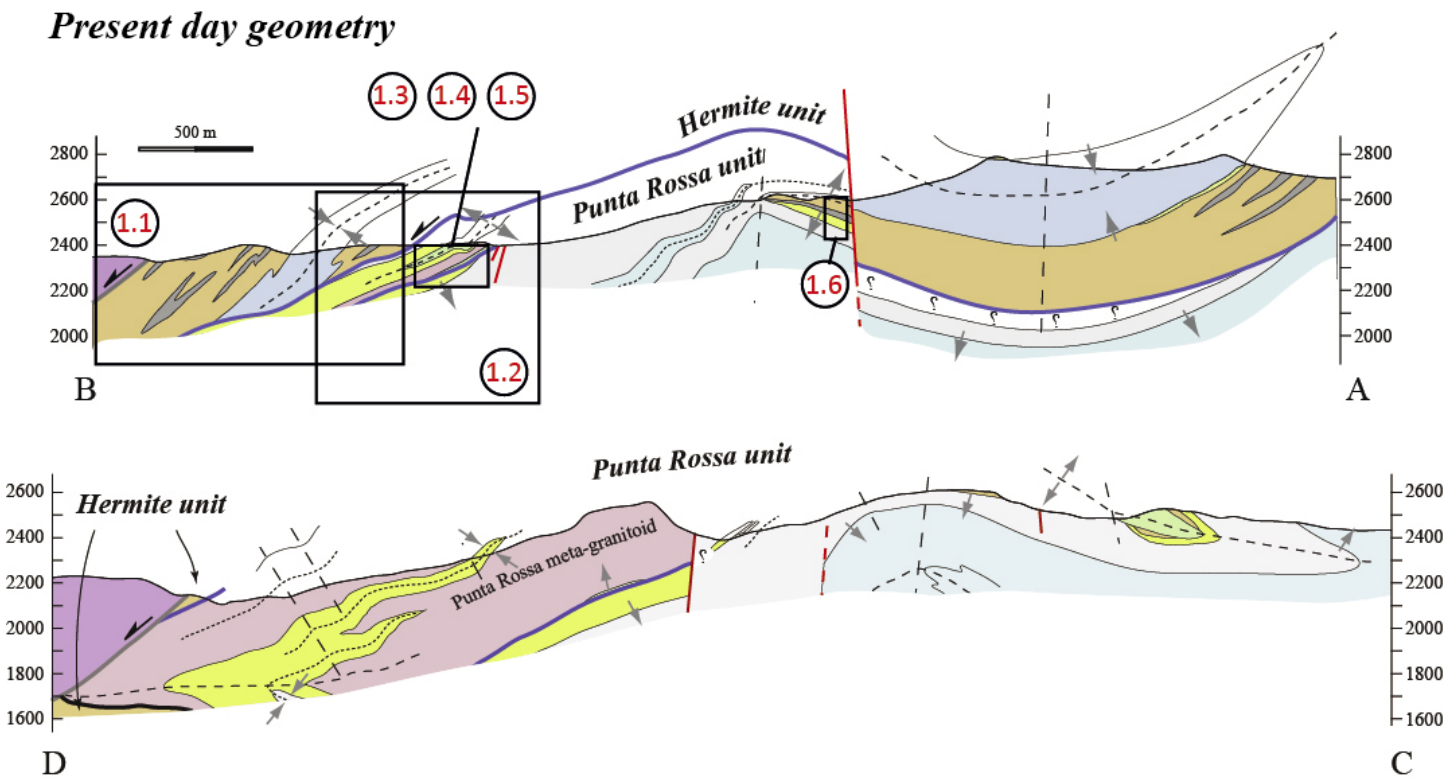

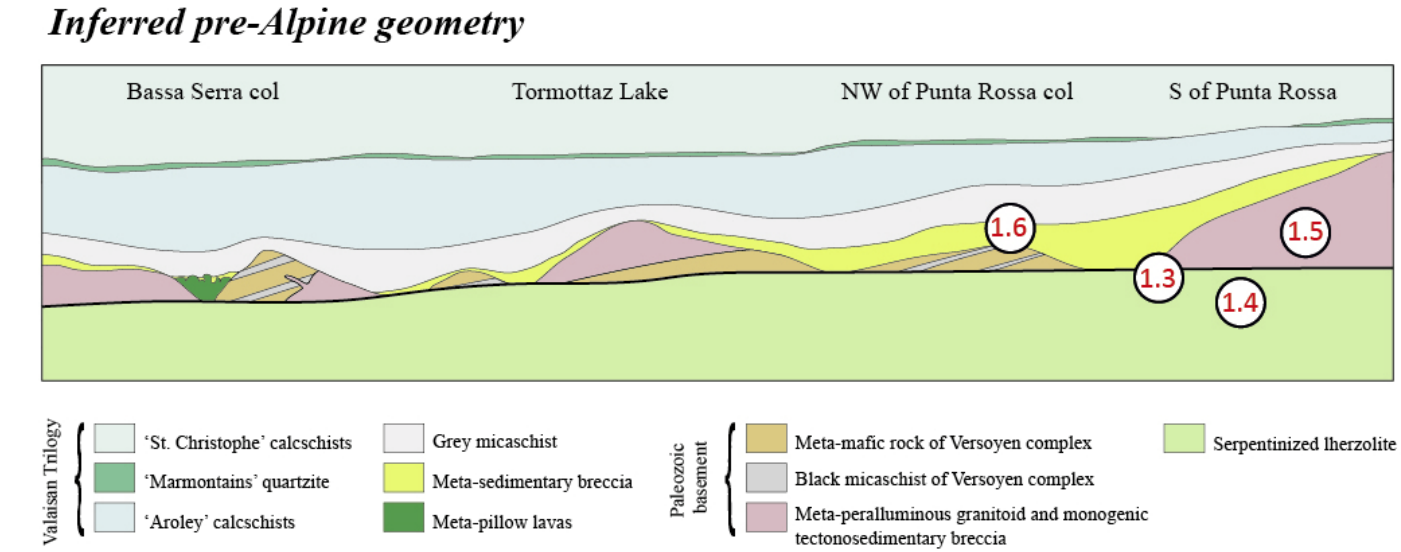

3.3.1 Ultramafic rocks, Paleozoic basement and Mesozoic pillow lavas

Serpentinized ultramafic rocks crop out throughout the Breuil Valley. The largest outcrops of serpentinized ultramafics are located near Punta Rossa (Stops 3 to 5) and further to the north, at Tormottaz Lake (Figs. 7 and 8). Serpentinite bodies display textural and mineralogical zoning, dependent upon the distance from the surrounding polymictic breccias and continental basement rocks.

Fig. 7 - Geological cross sections with excursion stops. Location of cross sections is indicated in Figure 6. Grey arrows indicate stratigraphic polarity. The pre-Alpine geometry, as inferred from structural and lithostratigraphic observations, is also depicted (from Beltrando et al., 2012).

DOI: 10.3301/GFT.2014.01

The significance of this zoning in terms of Jurassic and Tertiary evolution is discussed in Stops 1.3 and 1.4. Laterally discontinuous slivers of crystalline basement rocks are commonly associated with the ultramafic rocks (Figs. 5-8). Crystalline basement largely consists of leucocratic peraluminous metagranitoids (Fig. 9a), whose igneous protolith has been dated at 267±1 Ma (Beltrando et al., 2007). Paleozoic basement also consists of mafic–ultramafic sills and laccoliths interbedded with black schists, which are referred to as 'Versoyen complex' (Fig. 9b; Elter & Elter, 1965). Sills range in thickness from 0.5 to 40 m and locally show internal zoning, with cumulate gabbros and ultramafic layers passing upward to dolerites (Cannic, 1996). Chilled margins and intrusion breccias are common at the contact with the black schists (Beltrando et al., 2007). The cores of sills have flat REE patterns characteristic of N-MORB and T-MORB, while the geochemistry of the sill margins provides evidence for contamination caused by the intrusion of hot mafic magmas into unconsolidated sediments rich in water (Cannic, 1996 and Mugnier et al., 2008). As pointed out by Loubat (1975) and Kelts (1981), the Versoyen complex resembles sill–sediment complexes presently found in the Gulf of California, where they are related to high sedimentation rates during spreading within narrow oceanic pull-apart basins. Locally, metagranitoid dykes

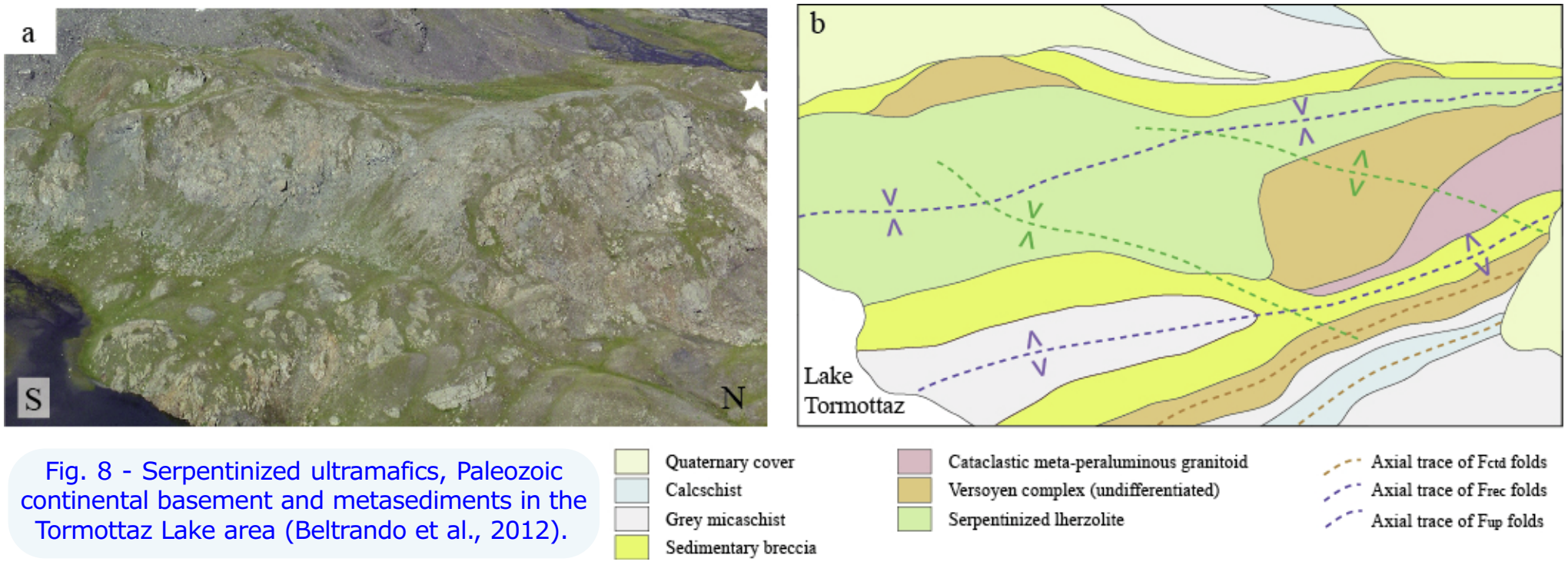

Fig. 8 - Serpentinized ultramafics, Paleozoic continental basement and metasediments in the Tormottaz Lake area (Beltrando et al., 2012).

DOI: 10.3301/GFT.2014.01

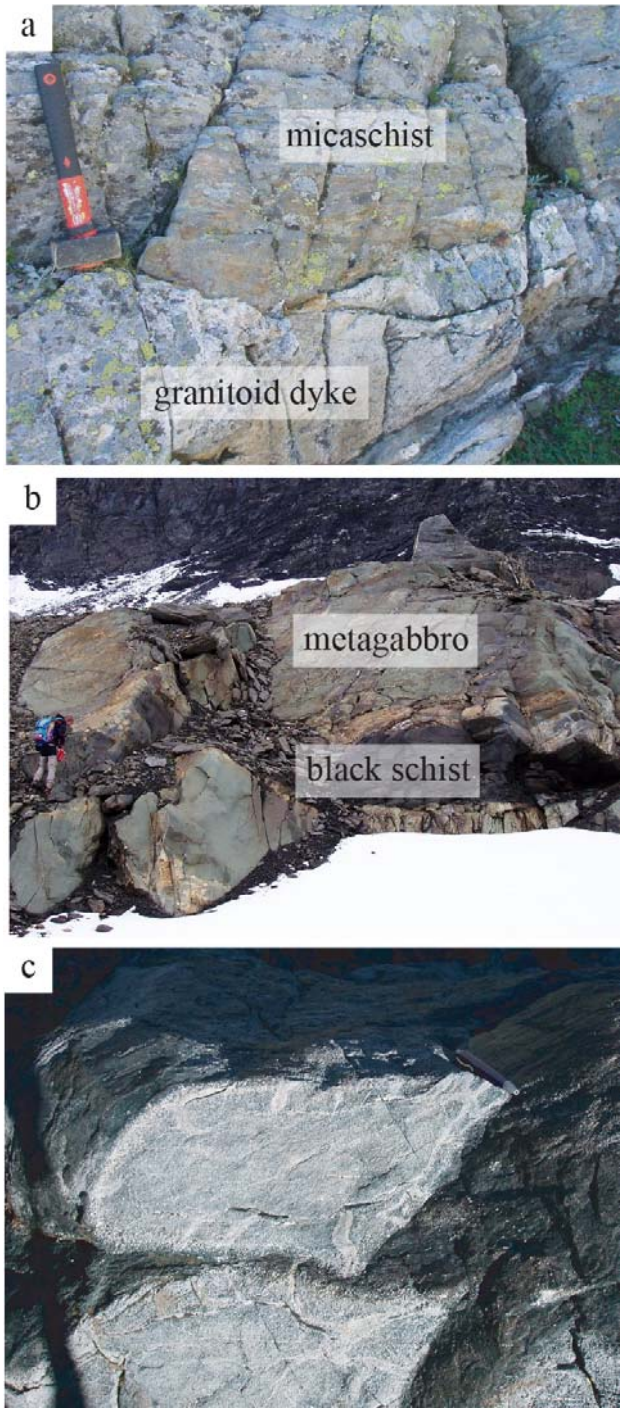

preserve intrusive relationships with black micaschists typical of the Versoyen complex, indicating that the latter is also Paleozoic (Fig. 9a).
Similar cross-cutting relationships are found in the neighboring Hermite unit (Schärer et al., 2000), where the Paleozoic age of the mafic magmas is also confirmed by U-Pb geochronology. Mafic magmatism was probably multi-stage, as the intrusion of a rather large mafic complex in the Aiguille de Clapet area (France) has been constrained at 337±4.1 Ma (Masson et al., 2008), while younger leucogabbro dykes were emplaced at 272±2 Ma (Beltrando et al., 2007).
Meta-pillowed lavas have been described from several localities within the Punta Rossa unit. Based on our observations, the only unambiguous evidence for basaltic lavas erupted at the seafloor is preserved near the Bassa Serra pass (Fig. 9c; Loubat, 1968; see Beltrando et al., 2012, for a discussion).

3.3.2 Metasediments

Serpentinized ultramafic rocks, Paleozoic basement and meta-pillow lavas are invariably associated with metabreccias, which contain clasts of all the lithologies described above. The lithological composition of this breccia is variable and is strongly controlled by the type of associated basement. Our structural study reveals that the meta-breccia outcrops found in the area were originally located along the same horizon (Fig. 7; Beltrando et al., 2012). The thickness of the metabreccia is variable, probably as a combined effect of pre-Alpine basin geometry and Alpine deformation. It ranges from a few meters, on the western side of Tormottaz Lake, where ultramafics and gray schists are separated by less than 5 m of polymictic breccia and meta-arkose, to about 20 m, on the ridge to the south-west of

Fig. 9 - Paleozoic basement consists mainly of meta-leucogranites **(a)**, locally intrusive into black micaschists. The black micaschists are generally associated with mafic sills **(b)**. Mesozoic pillowed metabasalts **(c)** are found near Bassa Serra Col.

DOI: 10.3301/GFT.2014.01

Punta Rossa. In the Punta Rossa area, where continental basement is rather homogeneous, differentiating between cataclastically deformed basement and re-sedimented monogenic breccia is often very difficult, due to the extensive Alpine deformation and metamorphism. As a result, we opted for grouping together tectonic and sedimentary monogenic breccias in the map presented in Fig. 6 under the 'tectono-sedimentary breccia' label. In all circumstances, the first unambiguous occurrence of sedimentary breccias is marked by the presence of polygenic breccias with a black matrix. Metabreccias often preserve transitional contacts with the underlying crystalline rocks and the overlying gray micaschists (Stop 1.6). Importantly, the "Collet des Rousses metabreccia", which is part of the Hermite unit and displays significant lithological similarities and identical stratigraphic position with respect to the metabreccias of the Punta Rossa unit, contains belemnites in the matrix, evidence for a Mesozoic depositional age.

The metabreccia is generally directly in contact with grey micaschists, consisting of graphitic schists that become progressively more carbonate-rich towards the (stratigraphically) overlying calcschists. Clasts of metagranitoids, metamafics and marbles are locally observed. The contact between carbonate-rich micaschists and the overlying calcschists is either gradational or characterized by interlayered calcschists.

A large part of the central and northern part of the Breuil Valley then consists of metasediments normally ascribed to the 'Valaisan trilogy' (Burri, 1979; Trümpy, 1951; see Masson et al., 2008 for a different view on the significance of these metasediments). From the contact with the gray micaschists, these metasediments are grouped in 'Aroley marble', 'Marmontains quartzite' and 'St. Christophe calcschists'. The Aroley marble consists of impure marble and carbonate schists, with rare conglomeratic beds near the base. The 'Marmontains quartzite' is characterized by alternating beds of carbonate-free black schists and quartzarenites, while the 'St. Christophe calcschists' consist of calcareous–arenaceous strata and black marls and schists. The onset of the Valaisan trilogy sedimentation is poorly constrained, due to the rarity of fossils, and it has been placed at different stages in the Cretaceous, either in the Barremian–Aptian (Elter, 1954; Sodero, 1968) or in the Turonian–Santonian (Antoine, 1965, 1971; see Loprieno et al., 2011 for a discussion).

3.4 Hermite unit

The Hermite unit consists of Versoyen complex rocks (e.g. Loubat, 1968), Collet des Rousses metabreccias and Arguerey calcschists (Antoine, 1971). In the Aiguilles de l'Hermite-Punta dei Ghiacciai area, aegirine and glaucophane rims are observed around magmatic clinopyroxene. The Collet des Rousses metabreccia is

DOI: 10.3301/GFT.2014.01

characterized by a laterally variable thickness and is locally absent at the Versoyen complex–Arguerey calcschist interface. The Arguerey calcschists consist of chlorite-white mica graphitic marble, phengitic micaschist, graphitic-carbonate paragreenstone, graphitic marble interlayered with chloritic marble and carbonate schist. Locally, the Arguerey calcschists contain rounded boulders of gray marble, which range in diameter from 30 cm to 1 m. For more details on the Hermite unit see Beltrando et al. (2012).

3.5 Tectono-metamorphic evolution

3.5.1 High pressure metamorphism

High pressure mineral assemblages are only rarely preserved in the Punta Rossa and Hermite units (Fig. 10): jadeite has been described in the Punta Rossa metagranitoids (Saliot 1979), carpholite is reported from metasediments of the Petit St. Bernard and Punta Rossa units (Bousquet et al., 2002; Goffé & Bousquet, 1997; Loprieno et al., 2011) and eclogites are locally preserved in large layered mafic complexes, which largely escaped exhumation-related deformation (Schürch, 1987; Cannic et al., 1996). Static re-equilibration of Paleozoic Fe-Ti-rich gabbros in the Hermite unit resulted into pseudomorphic replacement of omphacite (Jd_{50-55}) after augite, Ca-Fe rich garnet after plagioclase and rutile after ilmenite, variably associated with glaucophane 1 ± zoisite/clinozoisite ± quartz (Fig. 10; Cannic et al., 1996). Fe-Mg partitioning between co-existing garnet and clinopyroxene, which are never found directly in contact, combined with the phengitic substitution in rare white mica, yielded metamorphic conditions of P=1.4-1.6 GPa at T=425-475°C (Cannic et al., 1996). This temperature estimate lies at the upper limit of the maximum temperatures for metamorphism indicated by graphite crystallinity in Mesozoic and Paleozoic metasediments, falling in the 390-430°C range (Beltrando et al., 2012). Black micaschists of the Versoyen complex and grey micaschists of the Mesozoic cover are generally strongly re-equilibrated at lower-P conditions (see below), but rare lawsonite relicts have been observed (Cannic et al., 1996). In metasediments the carpholite + phengite + chlorite + quartz assemblage found in metamorphic veins has been estimated to have formed at P=1.5-1.7 GPa and T=350-400°C (Bousquet et al., 2002).

3.5.2 Post-high pressure tectono-metamorphic evolution

Post-high pressure metamorphism, in the metagabbros, is recorded by crystallization of a glaucophane 2 + zoisite/clinozoisite + phengite + paragonite + albite mineral assemblage, followed by re-equilibration at greenschist facies conditions, as indicated by the common assemblage actinolite-tremolite + albite + chlorite + Fe-epidote ±

DOI: 10.3301/GFT.2014.01

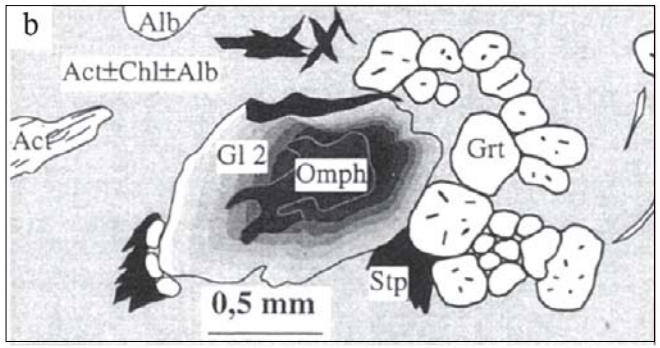

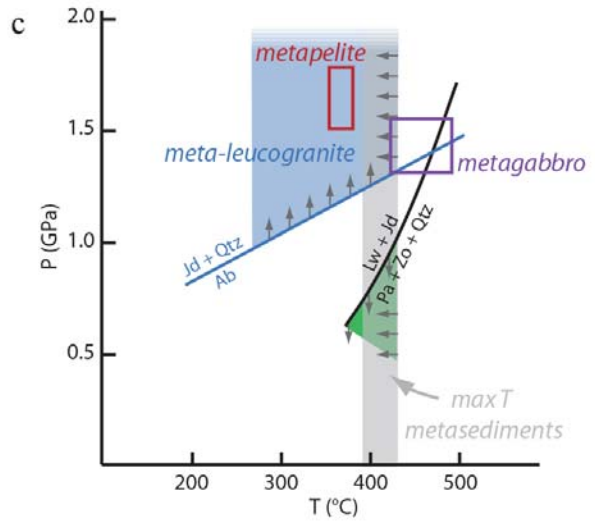

stilpnomelane ± pumpellyite (Cannic et al., 1996). Static greenschist facies retrogression is very pervasive in the relatively small mafic sills that will be observed during this excursion. Due to Alpine metamorphism, the mafic layers of the Versoyen complex now consist of albite–chlorite–actinolite bearing metamicrogabbros, albite–chlorite–epidote bearing metadolerites and greenstones, which only rarely preserve evidence of pre-existing glaucophane. As a result, the post-high pressure tectono-metamorphic evolution is best observed in the radiolaria-bearing grey micaschists, which preserve micro- and mesoscale evidence of the multistage post-HP deformation and metamorphic history (Fig. 11). In this lithology, relics of the HP evolution are restricted to (1) lozenge-shaped aggregates of muscovite, paragonite and chlorite, possibly derived from earlier lawsonite, (2) prismatic aggregates of chloritoid, quartz, white mica and chlorite, which may derive from former carpholite (Fig. 11a; Bousquet et al., 2002) and (3) a relict foliation, preserved in microlithons, defined by white mica with a high celadonite content (Si=3.4–3.5 a.p.f.u.). These relics are largely overprinted by a pervasive planar fabric, defined by white mica (Si=3.3 a.p.f.u.) and chloritoid, which is axial planar to isoclinal folds that affect the entire lithostratigraphy (F_{ctd} in Beltrando et al., 2012 and F1 in Fügenschuh et al., 1999 and Loprieno et al., 2011). The ubiquitous preservation of the original lawsonite and chloritoid porphyroclast shape is interpreted as evidence that their re-equilibration post-dated the formation of S_{ctd}. A second generation

Fig. 10 - High Pressure mineral assemblages are rarely preserved. Carpholite is locally found with quartz in metamorphic veins **(a)**, while omphacite relicts have been reported exclusively from the Clapet gabbro, in the Hermite unit (**b**, from Cannic et al., 1996). The PT estimates proposed for metamafics (Cannic et al., 1996) and for metapelites (Bousquet et al., 2002) are indicated by red and violet rectangles, respectively **(c)**. The minimum pressure of metamorphic re-equilibration of the metaleucogranite is constrained by the jadeite-in reaction. The maximum T of metamorphism is constrained by Raman thermometry (Beltrando et al., 2012).

DOI: 10.3301/GFT.2014.01

of chloritoid crystals is oriented at a high angle with respect to S_{ctd}, often associated to small garnet porphyroblasts, with a diameter <100 μm (Fig. 11a). *P*=1.3-1.5 GPa and *T*= 450-500°C have been proposed for the replacement of Fe-carpholite by chloritoid + chlorite + phengite (Bousquet et al., 2002). However, as noted above, the estimated temperatures greatly exceed those determined by thermometry based on Raman spectroscopy of carbonaceous material on the same metasediments (Beltrando et al., 2012). $^{40}Ar/^{39}Ar$ geochronology on metagranitoids and metasediments characterized by a pervasive S_{ctd} consistently yielded apparent ages in the 32.8-34.2 Ma range (Cannic, 1996), indicating that HP metamorphism was pre-Oligocene in age.
S_{ctd} is affected by mesoscale folds with rounded hinge, axial plane dipping to the west (270/40) and fold axis oriented NS (Fig. 11c). Such folding is associated with the formation of a new axial planar cleavage, with sub-mm to mm spacing, normally restricted to the hinge area. The new fabric is defined by white mica, chlorite, quartz and graphite and is labeled S_{rec} (where 'rec' indicates 'recumbent') in Beltrando et al. (2012) and F2 in Fügenschuh et al. (1999) and Loprieno et al. (2011). Folding is also responsible for deformation of the white mica aggregates developed at the expense of porphyroclastic lawsonite.

Formation of large-scale recumbent folds is followed by localized shearing along the Punta Rossa-Hermite units contact, which is slightly discordant with respect to the pre-existing lithological boundaries and to the axial planes of F_{ctd} and F_{rec}. Microscopic observations (Fig. 13c) indicate that the SE dipping chlorite-rich shear planes (labeled SZ_{SE} in Fig. 13), which are common within 2–4 m from the contact, cut across chlorite-rich pseudomorphs developed at the expense of former chloritoid. These observations are taken to indicate that top-to-the-southeast shearing took place at greenschist facies conditions. Late-stage shearing is then followed by large-scale upright folds (F_{up} in Beltrando et al., 2013 and F3 in Loprieno et al., 2011) characterized by steep axial planes and NNE–SSW to NE–SW striking fold axes (Fig. 11d). F_{up} folds are characterized by a box fold geometry and by relatively large along-axis strain gradient, resulting in significant variations in the fold amplitude. At the outcrop scale, F_{up} folds can locally be associated with a spaced axial planar cleavage restricted to a few outcrops to the north-west of the Tormottaz peak.
The overall architecture of the Hermite and Punta Rossa units, in the Breuil Valley, is mainly controlled by two large recumbent folds (F_{rec}/F2) deformed by an antiform-synform pair related to F_{up}/F3 (Fig. 7). The IEC excursion will take place on a limb of a major F2 fold, resting on the SE limb of the large F3 Tormotta anticline (Fig. 7). Therefore, in the area visited during the excursion, the effects of F2 and F3 are relatively minor and F1 folds can be observed, providing access to the oldest stages of the tectono-metamorphic evolution of the Valaisan domain.

DOI: 10.3301/GFT.2014.01

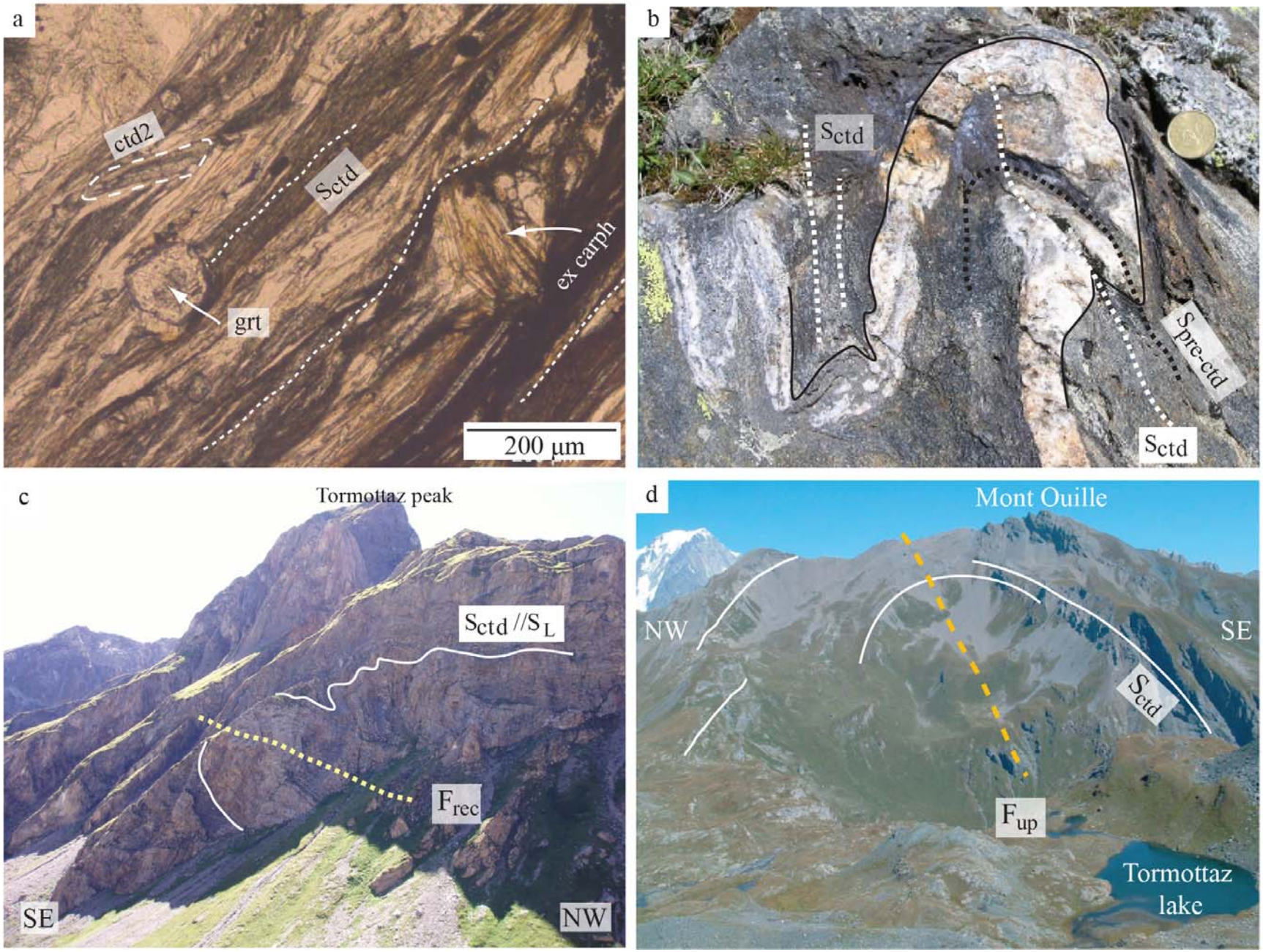

Fig. 11 - Tectono-metamorphic evolution recorded in grey micaschists. In this lithology the main fabric is marked by chloritoid and white mica and is axial planar to isoclinal folds (Sctd; **a, b**). This fabric wraps around relict carpholite and lawsonite and is statically overgrown by garnet and by a second generation of chloritoid. Sctd is then deformed by two main fold generations (**c** and **d**).

DOI: 10.3301/GFT.2014.01

DAY 2

4. UHP metamorphism of early post-rift sediments in the Lago di Cignana unit, Zermatt-Saas zone, Valtournenche

4.1 Geological setting

The ultrahigh pressure (UHP) Lago di Cignana unit (LCU) is exposed in the upper Valtournenche, Aosta Valley, Italian Western Alps (Figs. 3 and 18). The LCU is part of the Piemonte zone of calcschists with meta-ophiolites. It is considered to derive from the Jurassic Tethys Ocean, which separated the European continent from the Apulia (or Adria) plate (Fig. 4; Dal Piaz, 1974; Dewey et al., 1989; Polino et al., 1990; Lombardo et al., 2002 and references therein). In the upper Valtournenche, the Piemonte zone consists of a pile of tectonic slivers including both epidote–blueschist to lawsonite–blueschist facies (Combin zone) and eclogite facies (Zermatt–Saas zone) Alpine metamorphic rocks as defined by Bearth (1967). These two main ensembles of tectonic units of meta-ophiolites and metasediments are sandwiched between two continental crust units, the overlying Austroalpine Dent Blanche and the underlying Penninic Monte Rosa Massif (Fig. 3). The LCU is best exposed on the southern side of the artificial Lago di Cignana (Figs. 18, 19). Its small size, first recognized by Reinecke (1998), was later reduced by detailed mapping by Tamagno (2000) and Forster et al. (2004) (Fig. 19). The unit, which is <100 m thick, consists of 3 main slivers ~ 1000, 350 and 250 m long (Forster et al., 2004). It is overlain by a thin unit consisting of highly deformed metagabbro belonging to the Zermatt-Saas zone, which separates it from the overlying garnet-bearing metabasics. These metagabbros are alternatively considered as part of the Combin zone (Forster et al., 2004) or ascribed to the Zermatt-Saas zone, based on petrological and structural data (Pleuger et al., 2007; Groppo et al., 2009). Along its lower contact, the LCU is juxtaposed with a thick sequence of layered metagabbro and antigorite serpentinite of the Zermatt-Saas zone (Forster et al., 2004). Thus, the LCU is enclosed and enveloped by sheared tectonic slices derived from the Zermatt-Saas zone.

4.1.1 Deformation history/style

There is a number of remarkable aspects to the outcrops at Lago di Cignana when it comes to the style of deformation that can be observed. First all deformation that is observed in the Lago di Cignana rocks appears to have taken place during the exhumation. Everywhere, high pressure minerals have been intensely realigned

DOI: 10.3301/GFT.2014.01

during post-*P* peak deformation and recrystallization. Second it is evident that the rock mass has been boudinaged on all scales - from the kilometer scale, to the outcrop scale, to the microscope scale. In fact it is possible to map boudins within boudins within boudins. There is a history that can be discerned from these overprinting relationships, on the large scale in terms of relative timing, observing how the direction of motion changes, and on the microscope scale, using the combination of petrology, fabric and microstructural analysis, and microstructurally focussed $^{40}Ar/^{39}Ar$ geochronology to determine the temporal variation of pressure-temperature and process along the exhumation path. Boudins can be observed adjacent to the road, and the path leading down to the lake. The shear zones bounding these boudins are complex: for example the observed sense of shear can vary according to which side of a boudin is being observed. In the later part of the history the effect of some Alpine folding can be observed, with extensional boudins being folded and shortened. This is evident on outcrops near the lake shore.
At the map scale, due to this complex deformation history, slivers may be repeated at several different structural levels, attesting to the thrust-related movement involved at different times in this extensional setting. This is most evident when regarding the lithologies of boudins in the Combin Shear zone, which clearly come from a variety of different structural levels. These outcrops suggest what we have previously described (Forster et al., 2004; Lister & Forster, 2009) as a "tectonic shuffle zone" in this location. Alternatively, Beltrando et al. (2014) suggested that the apparent lithological complexity of the Combin Shear zone is largely inherited from pre-Alpine rift-related extensional tectonics, followed by subduction/exhumation-related shearing.

4.1.2 Main lithologies of the Lago di Cignana unit

The UHP unit consists of a basement of glaucophane eclogites with zoisite/clinozoisite + paragonite pseudomorphs after lawsonite, derived from original MOR basalts (cf. Groppo et al., 2009, Figs. 20, 21) and of a metasedimentary cover series. The metasedimentary sequence consists of four main lithologies, i.e.:

1. Glaucophane-garnet calc-micaschists and impure marbles with zoisite/clinozoisite + paragonite pseudomorphs after lawsonite, which include boudins and/or *nodules of quartz-bearing garnetite*. The eclogite peak assemblage consisted of aragonite (now calcite), coesite (now quartz), phengite, garnet, glaucophane, epidotes, lawsonite (now Zo/Czo + paragonite pseudomorphs), and accessory rutile, zircon, apatite and graphite.

DOI: 10.3301/GFT.2014.01

2. Omphacite-glaucophane-phengite-porphyroblastic garnet manganesiferous quartz-rich micaschists and quartzites with *nodules or boudinaged layers of garnetites, where microdiamonds have been discovered* (Frezzotti et al., 2011) (see below), and *jadeitite nodules*. The eclogite peak assemblage consisted of omphacite (now a Na-Ca amphibole-albite symplectite), glaucophane, phengite, coesite (now quartz), garnet, and lawsonite (now a Zo/Czo + paragonite pseudomorph).

3. Omphacite-garnet-glaucophane-chloritoid-lawsonite quartzites and quartz-rich schists with omphacitite nodules. The eclogite peak assemblage consisted of coesite (now quartz), omphacite-aegirinaugite, garnet, glaucophane, zoisite with allanite core, lawsonite (now Zo/Czo + paragonite), chloritoid, carbonate and accessory rutile, apatite, tourmaline, graphite and sulphides.

4. Piemontite-Mn-phengite-porphyroblastic garnet quartzites and quartz-rich micaschists with cm- to dm-wide black nodules. These nodules, which are most likely the sites of the original ferromanganese concretions of the ocean-floor, mainly consist of a mixture of Mn-Fe±Al oxides, garnets with a wide range of compositions of the spessartine-grossular±almandine solid solutions, minor carbonates (calcite, dolomite and rhodochrosite), pink Mn-bearing phengite, piemontite, talc and local tephroite (Mn-olivine), rutile, haematite, tourmaline, apatite and zircon.

4.1.3 The LCU metamorphic evolution

The manganiferous quartzites of LCU (see above, cover lithology 2), first described by Bearth (1967), have been later re-examined by Dal Piaz et al. (1979), but became well known among the students of ultrahigh-pressure metamorphism after the discovery by Reinecke (1991, 1998) of coesite included in a tourmaline crystal.

The first detailed petrographic description of the LCU unit has been given by Reinecke (1991), who studied the manganiferous quartzite. He found that garnet is zoned and that its mineral inclusions and chemical composition record the whole prograde, peak and retrograde evolution: primary quartz is included in the core and outer rim of the garnet, whereas only coesite is found in the inner rim. The peak metamorphic conditions have been inferred from the garnet inner rim, which is a pyrope-rich (up to Prp_{41}) spessartine coexisting with coesite, talc, kyanite, phengite, paragonite, braunite, piemontite, haematite, rutile, dravitic tourmaline, Mg-

DOI: 10.3301/GFT.2014.01

rich ardennite, apatite and zircon, recrystallized at high water activity. A similar history has been reconstructed also for eclogites by van der Klauw et al. (1997). Peak metamorphic conditions have been estimated at 615 ± 15 °C and 2.8 ± 1.0 GPa by Reinecke (1991, 1998) from metasediments and Reinecke et al. (1994) from basaltic eclogites. The exhumation history of the unit has been reconstructed on the basis of microstructural analysis of metabasics by van der Klauw et al. (1997). King et al. (2004) showed that garnet from eclogites preserves trace element evidence of prograde discontinuous reactions.

Recently, Angiboust et al. (2009), in a comprehensive study of the Zermatt-Saas unit eclogites through phase equilibrium modelling and Raman Spectroscopy of carbonaceous material, obtained homogeneous peak metamorphic conditions at about 540 ± 20 °C and 2.3 ± 0.1 GPa. Angiboust et al. (2009) suggested that the higher *PT* conditions estimated from the Lago di Cignana lithologies might be due: 1) to the detachment of a hm-scale tectono-metamorphic unit, later juxtaposed to the Zermatt-Saas ophiolites at 2.3–2.5 GPa; 2) to the lack of quartz inclusions within garnet or omphacite, which prevents the coesite formation; or 3) to minor non-lithostatic overpressure within the Lago di Cignana eclogitic unit, of the same order as those expected in the subduction channel from numerical experiments (c. 10%: Yamato et al., 2007; Raimbourg & Kimura, 2008). However, Groppo et al. (2009), studying in detail the metamorphic evolution of the meta-ophiolites of LCU and of the adjoining units, concluded that the peak assemblage garnet + omphacite + Na-amphibole + lawsonite + coesite + rutile formed at $T\sim$ 600 and $P>3.2$ GPa (Fig. 19), i.e. just within the diamond stability field (Day, 2012). These unusually high pressure conditions were later supported by Frezzotti et al. (2011), who discovered microdiamond inclusions in spessartine-rich garnets from the LCU quartzitic sedimentary cover. At temperatures of about 600°C, pressures conditions ≥ 3.2 GPa are also constrained by the graphite-diamond transition curve of Kennedy & Kennedy (1976). It should be noted, however, that the graphite-diamond transition curve has recently been modified and shifted to lower pressures (e.g., Fried & Howard, 2000; Day, 2012) compared to the one proposed by Kennedy & Kennedy (1976). Depending on which diamond-graphite transition curve is selected, minimum *P* conditions of diamond formation can vary between 2.8 and 3.2 GPa, at 600°C.

DOI: 10.3301/GFT.2014.01

4.1.4 Age of UHP metamorphism

Lu–Hf and Sm–Nd garnet geochronology by Amato et al. (1999) and Lapen et al. (2003) indicated ages of c. 50 and c. 40 Ma for the prograde and peak metamorphism, respectively. Slightly older ages of c. 44 Ma for the UHP peak metamorphism resulted from both *in situ* U/Pb dating of zircon by Rubatto et al. (1998) and $^{40}Ar/^{39}Ar$ high resolution laser dating of phengitic micas by Gouzu et al. (2006). Considering the previously published Sm–Nd and Lu–Hf geochronological data on a UHP eclogite, combined with the evidence that distinct core-to-rim zoning of different REEs in garnet of metamorphic rocks "record different times along a prograde growth history, and consequently may correctly interpret the isochron ages in terms of the garnet growth interval", Skora et al. (2009) concluded that prograde garnet growth occurred over a ~30 to 40 m.y. interval, i.e. garnet growth started at ~1.1 to 1.4 GPa pressure at ~70 to 80 Ma ago and peak metamorphism occurred at 38 to 40 Ma ago.

4.2 The impure quartzite and the manganiferous garnetite

The *impure quartzites* including manganiferous garnetites consist of quartz, garnet, minor phengite, partly chloritized green-brownish biotite, piemontite and accessory rutile, opaque ores (most likely Mn-oxides), apatite and a slightly zoned pale green tourmaline. More than one generation of white mica may be recognized based on microstructural position, grain size and interference color. The pale pink manganoan phengite (Reinecke, 1991) crystallized with the uniaxial 3T polytype. The bimodal arrangement of phengite crystals and the local presence of isoclinal fold hinges within the main foliation indicate that the latter was formed through transposition of an older fabric. In the most retrogressed sites, phengite is pseudomorphically replaced by albite. Tourmaline occurs locally as slightly zoned phenoblasts which include piemontite, rutile and opaque ores. Apatite is typically cloudy for the presence of tiny needle-like opaque segregations, elongated parallel to the host crystal c-axis. Rare clinozoisite crystals also occur, usually oblique to the main foliation, with a pale purple radioactive core. Piemontite is often surrounded by a pale yellow green rim of clinozoisite.

The original *manganiferous garnetite* occurs in quartzite as a few cm-thick discontinuous layers, knots or nodules pink to red-brown in colour that appear to have formed by boudinage of an original layer (Fig. 22). Locally, nodules appear to be hinges of rootless isoclinal folds. Garnetite consists of an inner portion of massive, close packed, equigranular aggregate of small (c. 50-300 μm across) welded garnets and accessory

DOI: 10.3301/GFT.2014.01

rutile and apatite. Only in places a thin film of quartz is present among garnet granoblasts. The original almost monomineralic garnetite is usually dismembered into fragments with angular shapes separated and cemented by a network of fractures healed with quartz (Fig. 23 left). Locally, this quartz appears to be recrystallized to poikiloblasts up to more than c. 2 cm across, which show a subgrain microstructure whose grain size is similar to that of the surrounding quartzite. Moving further away from the garnetite core, the quartz-garnet ratio increases, but the shape of the nodule is usually still preserved.
Even if the manganiferous garnetite lenses of the LCU are similar to coticule or pseudocoticule from the Belgian type locality (Baijot et al., 2011), they differ as to both the mineral mode and composition. However, it cannot be excluded that the LCU garnetites may have derived from sediments deposited onto the oceanic crust, consisting of radiolarian ooze impregnated with halmyrolized (halmyrolization = a kind of submarine weathering) Mn-rich oxides and/or carbonates together with a clay fraction. The possible derivation of spessartine from a rhodochrosite precursor, suggested by Lamens et al. (1986), has been confirmed by Schreyer et al. (1992).

4.2.1 Garnets of garnetite

In the massive garnetite, where garnets show a granoblastic microstructure and are welded together, each single garnet crystal may be recognized only because the presence of the reddish core rich in inclusions surrounded by a colourless rim. In the more dismembered portions of garnetite single garnets are cemented by intergranoblastic quartz, each garnet consisting of a reddish core usually rich in inclusions of opaque and carbonates, and a colourless inclusion-free or inclusion-poor rim (Fig. 23 left). Locally, garnets may exhibit an atoll-like habit, consisting of a reddish core rich in inclusions with corroded appearance, and a colourless idioblastic rim. Core and rim are separated by a quartz mantle. However, different types of shape and zoning may be observed (Fig. 23 right).

4.2.2 Inclusions in garnet of garnetite

Garnet cores are usually rich in inclusions of opaque, quartz/coesite magnesite, and dolomite (Fig. 23). Mineral inclusions range in size from 40 to 200 μm and show rounded or elongated shapes. Coesite and quartz are commonly present as single crystals, and the usual petrographic features associated with the coesite-quartz transition are lacking (i.e. visible coesite relic; palisade-textured quartz; polygonal granoblastic quartz

DOI: 10.3301/GFT.2014.01

aggregate). Garnet contains also rare microdiamond inclusions. Microdiamonds range from 1 to 20 μm in size, with an average size of 2-6 μm. They are blackish, subhedral to euhedral, and often show well developed octahedral and cubic shapes. Microdiamonds are always associated with carbonates and fluid inclusions (i.e. coeval). Metamorphic graphite has not been observed. Diamond cubic structure (i.e. C-C bonding of sp^3-hybridized C) was confirmed by a sharp band at 1332 (± 2) cm^{-1} in the Raman spectra. All diamond bands from a data set of more than 40 spectra show high crystallinity with a Raman band spread of 3.5 - 7.6 cm^{-1} FWHM (full with at half peak maximum intensity). Water-rich fluid inclusions (Fig. 23; 2-30 μm in size) associated with microdiamonds contain several daughter crystals, including Mg-calcite/calcite, quartz, rutile, paragonite ± dawsonite ± rhodochrosite ± hydrous Mg-carbonate and sulfate (e.g., dypingite $Mg_5(CO_3)_4(OH)_2 \bullet 5H_2O$, and pentahydrite $MgSO_4 \bullet 5H_2O$).
Raman microspectroscopy detected bicarbonate, sulfate, carbonate ions (peaks at 1017, 981, and 1066 cm^{-1}, respectively), and H_4SiO_4 monomers and dimers in the aqueous solution (Frezzotti et al., 2011). Raman failed to detect CO_2 in gas bubble, constraining the mole fraction of CO_2 in the fluid phase to be < 0.026.

DOI: 10.3301/GFT.2014.01

Day 1: Punta Rossa unit (Valaisan domain)

STOP 1.1 - Alpine architecture: The Punta Rossa-Hermite-PSB stack

(Coord.: Long: 6.870780 E; Lat: 45.695840 N)

This first Stop is located along the main track, in the flat meadow after a calcschist cliff. This stop is aimed at illustrating the overall tectonic architecture of the area. The Petit St. Bernard, Hermite and Punta Rossa units are stacked along south-dipping contacts and the Petit St. Bernard unit occupies the southernmost position (left in Fig. 12). The contact with the underlying Hermite unit is marked by a sharp shear zone dipping to the south, which is locally marked by cargneule, tectonic breccias with angular clasts in a yellow calcite matrix. An extensional crenulation cleavage is commonly found in the black micaschists and in the Arguerey calcschists of the Hermite unit, in the footwall, indicating that this tectonic contact was characterized by top-to-the-south

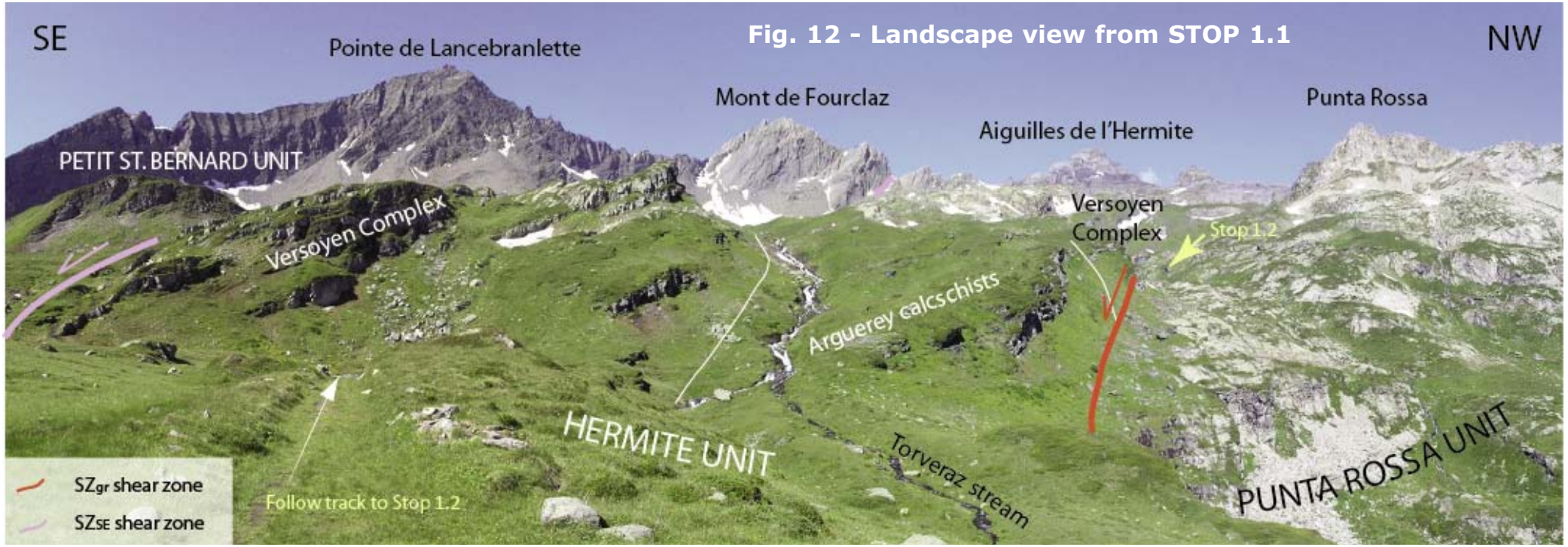

Fig. 12 - Landscape view from STOP 1.1

DOI: 10.3301/GFT.2014.01

kinematics (Cannic et al., 1995; Beltrando et al., 2012). The lower boundary of the Hermite unit can be seen at the base of the grassy slope above the grey-greenish outcrops of the Punta Rossa metagranite. From this viewpoint, all the different lithologies of the Hermite unit can be observed. The Versoyen complex, with the characteristic banded appearance related to the green-gray mafic sills and the black schists, can be seen both in the cliffs to the left and on the top of the Aiguille de l'Hermite. The base of the Aiguilles de l'Hermite, as seen from here, consists of Collet des Rousses conglomerates, resting on the overturned limb of a large F_{rec}/F2 fold. Please, note that also this metasedimentary formation is banded and, from a distance, can hardly be distinguished from the Versoyen complex. Collet des Rousses conglomerates crop out also in the foreground, in the cliff directly above the Punta Rossa unit. The Arguerey calcschists, instead, crop out both in the grassy slope in the foreground and on the north-eastern ridge of the Aiguille de l'Hermite. Observations along the Torveraz streambed, in an area not visible from here, indicate that the Arguerey calcschists rest in the core of a tight antiform (Figs. 6 and 7), with axial planar cleavage in the black schists defined by elongated chloritoid and white mica. This fold generation is ascribed to F_{ctd} by Beltrando et al. (2012), which corresponds to F1 in Fügenschuh et al. (1999) and Loprieno et al. (2011). The lower limb of this tight fold, towards the contact with the underlying Punta Rossa unit, is dissected and partly dismembered by minor shear zones (not visible from here). As already mentioned above, the Punta Rossa unit rests directly underneath this late-stage tectonic contact, which will be seen in Stop 1.2. The serpentinites (green) can already be spotted in the rocky ridge in the middle of the picture.

STOP 1.2 - Contact between Punta Rossa and Hermite units

(Coord.: Long: 6.862320 E; Lat: 45.697590 N)

Before looking at the internal architecture of the Punta Rossa unit, which is the main topic of this excursion, one more stop is devoted to the understanding of the overall architecture of the area and the contact with the Hermite unit. Stop 1.2 is located along the main track leading towards the Punta Rossa pass, a few tens of meters above the marsh. A view to the south, to the streambed and the cliff lying behind it, allows introducing some of the main lithologies of the Punta Rossa unit, where the Paleozoic basement is overlain by Mesozoic sediments (Fig. 13). The bottom of the valley, floored by pale greenish rocks, consists of metagranitoids, locally preserving the original igneous mineral assemblage, consisting of sub-cm sized quartz, plagioclase and K-feldspar, now largely replaced by aggregates of albite and fine grained white mica. White mica inclusions found

DOI: 10.3301/GFT.2014.01

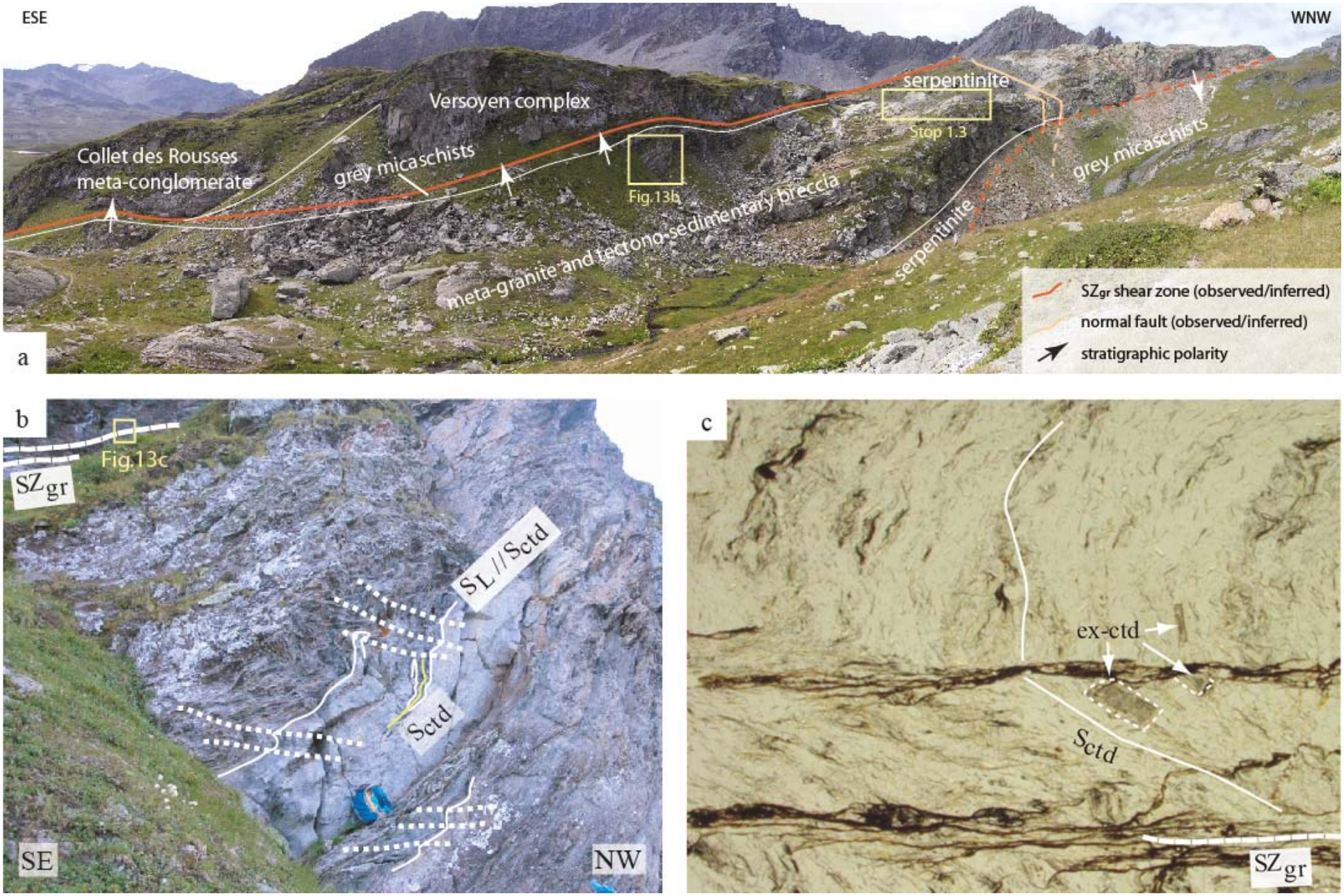

Fig. 13 - Landscape view from STOP 1.2 **(a)** and main features of the Punta Rossa grey micaschists in immediate footwall of the contact with the overlying Hermite unit (**b** and **c**).

DOI: 10.3301/GFT.2014.01

in sub-cm sized magmatic relicts of quartz and plagioclase suggest that the Punta Rossa metagranitoid originated from a Si-rich, most likely peraluminous, magma. An original albitic composition for the plagioclase is suggested by the lack of epidote or other Ca-bearing phases. The sample of leucocratic metagranite that was studied by U-Pb geochronology by Beltrando et al. (2007) was collected just outside the field of view of this picture, to the left, along the main track descending into the valley. Magmatic zircon cores yielded an age of 267±1 Ma, interpreted as the timing of magma crystallization (Beltrando et al., 2007). Metamorphic white mica, in the rock matrix, defines a relict foliation in microlithons bounded by a spaced foliation defined by neoblastic white mica. This pervasive fabric is sub-parallel to the main lithological boundaries and to the S_{ctd} fabric (S1 in Loprieno et al., 2011) in the overlying grey micaschists (see below). Pervasive post-S_{ctd} re-equilibration under greenschist facies metamorphic conditions is indicated by the static growth of large albite porphyroblasts.

As discussed in the 'Geological Setting', in this domain, as in most of the area, it is generally very difficult to distinguish between pristine metagranitoids, cataclastic metagranitoids and re-sedimented monomictic metagranitoid conglomerate. The granitoid grades westward (to the right, in the Fig. 13) into a polymictic breccia (which will be seen in Stop 1.3), consisting of clasts of granitoids analogous to those of the Punta Rossa body, together with micaschists. The white-greenish cliffs with the brown streaks rising rightward from the marsh area consist mainly of this polymictic breccia. The grassy slope behind the breccia hosts banded metamafics, metapelites, meta-arkose layers, grading upward into a grey micaschist (Fig. 13b). The lithological contacts and the S_{ctd} fabric, characteristic of this granitoid/breccia/meta-arkose/grey micaschist sequence, are truncated by a slightly discordant, sharp, south-dipping shear zone (Fig. 13a). In the proximity of the contact, within a distance of ca. 10 meters from the overlying Versoyen complex rocks belonging to the Hermite unit, lithological contacts and S_{ctd} are deformed by asymmetric open folds with rounded to sharp hinges and discontinuous axial planes (Fig. 13b). These folds are interpreted as related to syn-shear folding of originally steeper planar surfaces during top-to-the-south extensional shearing. Microscopic observations indicate that the SE dipping chlorite-rich shear planes, which are common within 2–4 m from the contact, which dips 20-25° to the SSE, cut across chlorite-rich pseudomorphs developed at the expense of former chloritoid (Fig. 13c). These observations indicate that top-to-the-southeast shearing took place at greenschist facies conditions.
An important aspect to note in this Stop concerns the lithological composition of the Punta Rossa unit visible from here, which is common to the rest of the Breuil Valley. Paleozoic basement, here consisting of variably

DOI: 10.3301/GFT.2014.01

cataclastic peraluminous metagranitoids, is juxtaposed to monomictic breccias, polymictic breccias and to finer grained meta-arkose-metapelite and grey metapelites. The gradual transition from Paleozoic basement to a clast-supported monomictic breccia, to a matrix-supported monomictic breccia to the radiolaria-bearing grey micaschist can be observed in several parts of this field area, such as to the north of the Punta Rossa pass (Stop 1.6). The analogy with the lithostratigraphy observed here indicates that, in this location, we are looking at a 'right-way-up' transition from Paleozoic basement to Mesozoic sediments. Instead, in the rest of the area, grey micaschists lie below the Paleozoic basement and polymictic breccia, which are found in the cliff to the right in the picture. (Overturned) gradational contacts between breccias, arkosic-pelitic metasediments and radiolaria-bearing gray micaschists are preserved along the track leading to the Punta Rossa pass. In the cliffs visible to the right of this field of view, instead, this inverted stratigraphy is affected by minor reactivation along shear planes dipping ca. 40° to the SE, sub-parallel to the Punta Rossa-Hermite unit contact. The change of stratigraphic polarity from the cliff underneath the Hermite-Punta Rossa contact to the rest of the Breuil Valley is related to a tight F_{ctd}/F1 fold, with axial plane dipping to the south, parallel to S_{ctd}. Parasitic folds related to this major structure are locally seen in the Punta Rossa metagranitoids. The serpentinized ultramafics that will be visited in the next stop are located within the hinge of this F_{ctd}/F1 synform.

STOP 1.3 - A paleo-ocean floor: the contact between ultramafic rocks and metasedimentary breccia

(Coord.: Long: 6.860130 E; Lat: 45.696210 N)

After descending back to the marsh area, head SW-ward, leaving the track and walking along the base of the slope hosting the contact between the Punta Rossa and Hermite unit. The banded meta-mafic/metapelite sequence lying at the base of the grey micaschists can be reached with a small detour on the grassy slope (very slippery when wet). In the largest cliff, the interference between F_{ctd} folds and the shear-related folding can be observed (Fig. 13b). From this point, start ascending to the SW, between the boulders until the first outcrops, consisting of glacier-polished polymictic breccias, which are variably deformed. This Stop is devoted at illustrating the key features of the ultramafics-polymictic breccia contact in a small area, extending to the slope just above the small lake. This Stop will also give us the chance to discuss the different sets of observations that are necessary to assess whether a specific lithological contact or lithostratigraphic unit was assembled during subduction-related tectonics as opposed to pre-subduction rifting.

DOI: 10.3301/GFT.2014.01

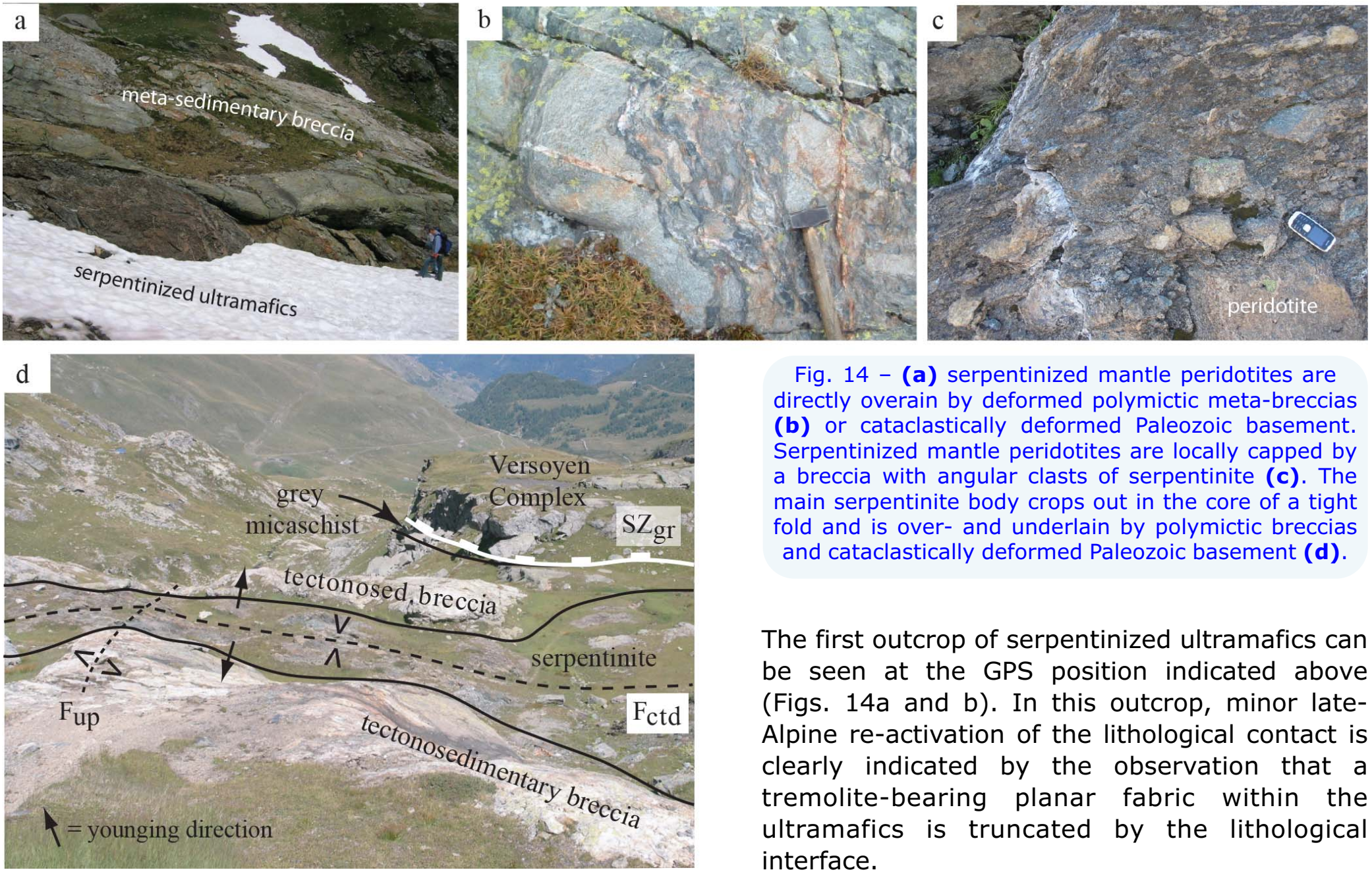

Fig. 14 – **(a)** serpentinized mantle peridotites are directly overain by deformed polymictic meta-breccias **(b)** or cataclastically deformed Paleozoic basement. Serpentinized mantle peridotites are locally capped by a breccia with angular clasts of serpentinite **(c)**. The main serpentinite body crops out in the core of a tight fold and is over- and underlain by polymictic breccias and cataclastically deformed Paleozoic basement **(d)**.

The first outcrop of serpentinized ultramafics can be seen at the GPS position indicated above (Figs. 14a and b). In this outcrop, minor late-Alpine re-activation of the lithological contact is clearly indicated by the observation that a tremolite-bearing planar fabric within the ultramafics is truncated by the lithological interface.

DOI: 10.3301/GFT.2014.01

The sliver of ultramafics rests in the core of an F_{ctd}/F1 fold (Fig. 14d), with the normal limb preserved in the south-eastern part of the area and an inverted limb in the slopes immediately above the small lake, where serpentinites are underlain by metabreccias. These folds are themselves deformed by open fold with steep axial planes and NE-SW trending fold axes. Older fold generations can be observed within the ultramafic body, but their correlation with pre-F_{ctd} folds seen elsewhere in the grey micaschists (Fig. 11b) is prevented by the pervasive F_{ctd} overprint, by the greenschist facies retrogression common in the micaschists and by the absence of a distinctive syn-kinematic mineralogy in the ultramafic rocks.

Following the serpentinite-metabreccia interface from the first outcrop for a few tens of meters, reach a new footpath and follow it for a few tens of meters to the WSW. In this location, the ultramafic rocks consist of a clast-supported breccia, with angular clasts ranging in size from a few cm to several tens of centimeters (Fig. 14c). Development of an Alpine mineral fabric is generally restricted to the breccia matrix. The position of this ultramafic breccia, at the interface between massive serpentinized ultramafics and polymictic breccias/cataclastic Paleozoic basement, suggests that it marks the original exhumation surface of this ultramafic body at the basin floor, in the Mesozoic. Pervasive Alpine deformation prevents assessing whether this breccia originated as a cataclasite along an exhumation fault or as a monomictic sedimentary breccia.

The outcrops to the SE of this ultramafic breccia preserve further examples of the metasedimentary breccia resting directly in contact with serpentinite. Descending towards the lake, an outcrop of white 'metagranitoids' reveals, at a closer inspection, its origin as a monomictic sedimentary breccia, consisting exclusively of clasts of leucocratic granitoid similar to the Punta Rossa metagranite. This outcrop serves as a vivid illustration of the difficulties involved with distinguishing among preserved basement, cataclastic basement and resedimented basement in areas affected by multiple stages of subduction-related deformation/metamorphism.

STOP 1.4 - Serpentinized spinel peridotite

(Coord.: Long: 6.855600 E, Lat: 45.694470 N)

Walk up the grassy slope to the WSW, past the polymictic breccia on the inverted limb of the F_{ctd} fold, until reaching a NE-SW trending break in the slope, hosting small ponds, related to minor SE-dipping high-angle faults (Fig. 13). These late-Alpine faults bound the ultramafic rocks, which here preserve their pre-hydration

DOI: 10.3301/GFT.2014.01

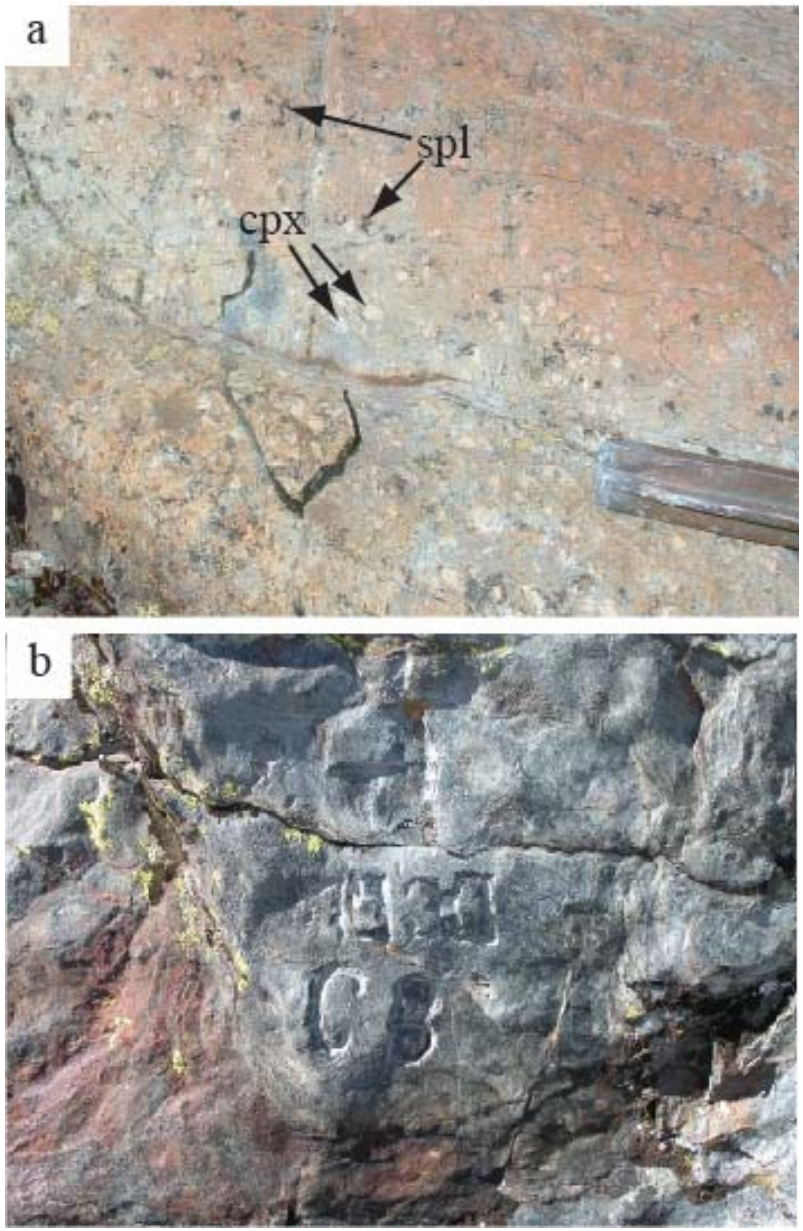

Fig. 15 – **(a)** serpentinite preserving the original mantle peridotite texture; **(b)** chloritite quarry.

mineral texture and (occasionally) mineralogy (Fig. 15a). Comparison of this outcrop with the ultramafic rocks seen in the previous stop clearly indicates that the serpentinite body is texturally and mineralogically zoned, depending upon the distance from the surrounding polymictic breccias and continental basement rocks. At a distance >10 m from other lithologies, the texture of the pre-existing spinel lherzolite is generally preserved, with a weak foliation defined by the original spinel and cm-sized clinopyroxene (Fig. 15a), now largely replaced by aggregates of tremolite ± antigorite. Rare cpx is the only relict of the original peridotitic mineral assemblage, while both orthopyroxene and olivine are completely replaced by brucite and interlocking antigorite. Relicts of the peridotite texture disappear within a few meters from the contact with the polymictic breccia, where the massive serpentinite is locally replaced by a clast-supported tectonic breccia with variably sized angular clasts (Stop 1.3) largely consisting of antigorite, associated with tremolite + talc + rare carbonates.

Following this narrow NE-SW break in slope to the SW, we reach the inverted limb of the F_{ctd} fold, where the contact between ultramafics and cataclastic continental basement is marked by several centimeters of chloritite. This metasomatic rim was quarried in the past to build baking stones (Fig. 15b).

DOI: 10.3301/GFT.2014.01

STOP 1.5 - The contact between continental basement and ultramafic rocks: pre-metamorphic brittle deformation and alpine metasomatism

(Long: 6.855810 E, Lat: 45.695350 N)

Climbing uphill to the right of the chloritite quarry, small outcrops of ultramafics rest above cataclastic basement and polymictic breccias, as a result of the interference between F_{ctd}/F1 and F_{UP}/F3 folds. Typical characteristics of the Paleozoic basement can be seen on a sub-horizontal outcrop surface, directly below a klippe of ultramafics (Fig. 16a). Here, angular polymineralic clasts of leucocratic granite, analogous to the Punta Rossa basement, are wrapped around by dark foliated layers, largely consisting of white mica + chlorite (Fig. 16b). Similar lithologies are found in the Tormottaz Lake area (Beltrando et al., 2012), where angular polymineralic clasts ranging in size from a few millimeters to 3–4 cm, are wrapped around by a dark matrix, giving rise to a mesoscale texture typical of a fault breccia with mm-thick gauge layers (Fig. 16c). However, no evidence of brittle deformation is preserved at the microscopic scale, since the dark matrix hosts a chlorite + white mica fabric post-dating glaucophane and lawsonite porphyroclasts (now replaced by albite + chlorite aggregates and white mica + chlorite + epidote aggregates, respectively; Fig. 16d). These observations indicate that cataclastic deformation predated the oldest metamorphic fabric seen here (S_{ctd}/S1). Based on their position, at the interface between serpentinized ultramafics and continental basement, and on the overall lithostratigraphy of the Punta Rossa unit, these cataclasites are interpreted as Mesozoic fault breccias.
A short hike to the top of the ultramafic klippe provides a general view of this part of the Western Alps, with the little metamorphosed Houiller zone on the slopes behind the road leading to the pass, resting on top of the Houiller Front, which runs along the main valley, between the Petit St. Bernard Col and La Thuile. This tectonic contact marks a major metamorphic gap, as the rocks found in the immediate footwall (Petit St. Bernard unit, Hermite unit, Punta Rossa unit) experienced $P \geq 1.5$ GPa during the Alpine orogeny and temperatures in the 400-450°C range (Bousquet et al., 2002; Loprieno et al., 2011; Beltrando et al., 2012), while the Houiller zone underwent Alpine metamorphism at $P = 0.6 \pm 0.2$ GPa and $T = 280$-300°C; Lanari et al., 2012).

DOI: 10.3301/GFT.2014.01

STOP 1.5

Tormottaz Lake

Err Nappe

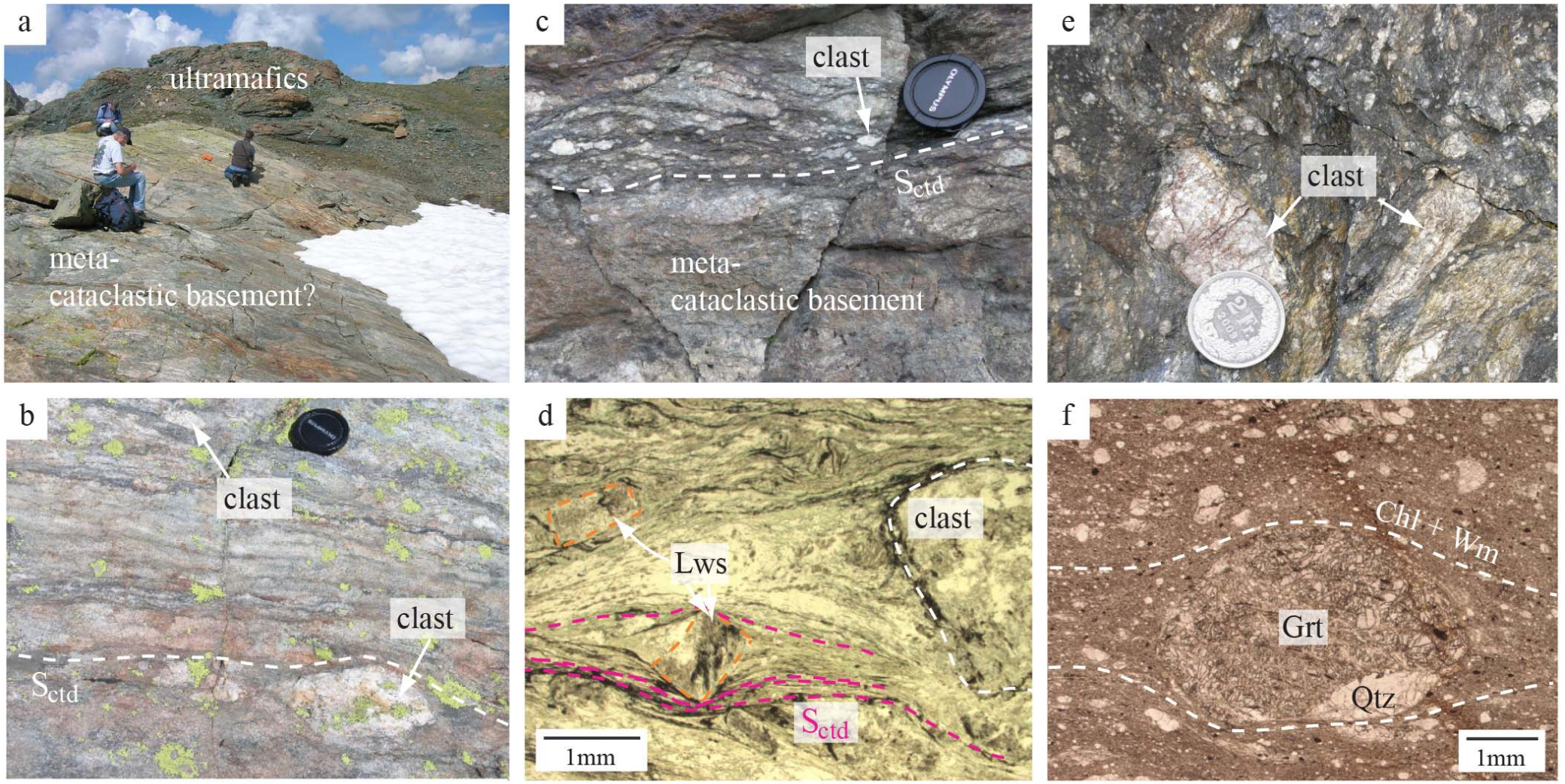

Fig. 16 – The metamorphosed continental basement, which crops out structurally underneath the serpentinized ultramafics (**a**, **b**), displays several features analogous to the meta-cataclastic basement of the Tormottaz Lake area (**c**, **d**), which in turn can be compared to the Jurassic fault gauge of the Err detachment, in the Eastern Alps (**e** and **f**; figure **e** was kindly provided by G. Manatschal).

DOI: 10.3301/GFT.2014.01

STOP 1.6 (optional) - (Overturned) stratigraphic transition between Paleozoic basement, Mesozoic breccia and radiolaria-bearing garnet-chloritoid micaschist

Visit to this Stop involves an extra 30 minute hike uphill from Stop 1.5. This Stop provides further constraints on the Alpine architecture of the Punta Rossa unit and on the pre-Alpine basement-cover relationships. Furthermore, this Stop provides the opportunity to sample the radiolarian-bearing garnet-chloritoid micaschists described in Beltrando et al. (2012). The hike to this stop follows the main ridge to the NW, up to a NE-SW trending depression, hosting small ponds and a larger lake to the NE. Upon reaching this lake, climb up the slope to the NW, within grey micaschists and calcschists, reaching a NE-SW trending rounded ridge, which corresponds to the axis of a major F_{UP}/F3 antiform. On the northern limb of this antiform a short west-to-east walk crosses the (overturned) contact between Paleozoic basement and Mesozoic sediments. Metagabbros and black micaschists of the Versoyen complex are directly underlain by a clast-supported breccia consisting of angular clasts of metagabbro. The matrix/clast ratio increases towards the east, where occasional clasts are found within the grey micaschists, which are then underlain by calcschists (Fig. 17). This gradual transition from Versoyen complex to breccias and grey micaschists is interpreted as an overturned contact between Paleozoic basement and its autochthonous sedimentary cover. This relationship is similar to the one described in Stop 1.2, where the Paleozoic basement, there consisting of peraluminous granitoids, was overlain by a sedimentary breccia with abundant granitoid clasts, followed upward by grey micaschists. The polarity change is due to F_{ctd}/F1 folding, as most of the Punta Rossa unit, in the Breuil Valley, rests on the inverted limb of a major F_{ctd}/F1 synform and in the long limb between large-scale F_{rec}/F2 recumbent folds [which have not been shown in this excursion (for details see Beltrando et al., 2012)]. The radiolarian-bearing garnet-chloritoid micaschists can be sampled here. Please note that similar rocks are found throughout the grey micaschists. The radiolarian-bearing gray micaschists, at the meso- and microscale, are characterized by a pervasive S_{ctd} fabric, defined by white mica (Si=3.3 a.p.f.u.) and chloritoid (S_{ctd}; Fig. 17). A second generation of chloritoid crystals is oriented at high angle with respect to S_{ctd}, often associated with small garnet porphyroblasts, with a diameter <100 μm. Microfossils are commonly found within this lithology. Their preservation was probably related to diagenetic pyritization, which occasionally retains the original skeleton internal structure.

DOI: 10.3301/GFT.2014.01

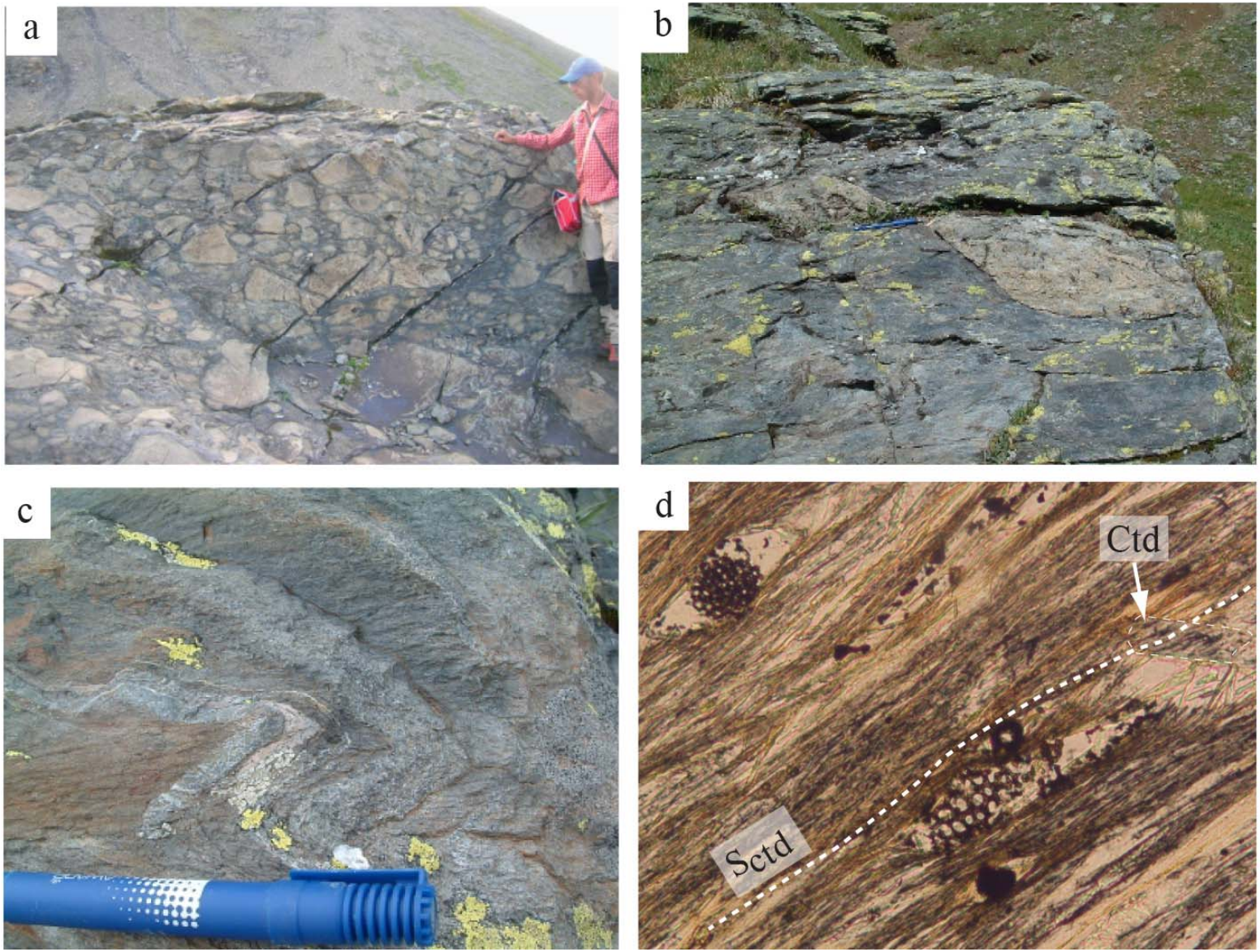

Fig. 17 – The gradual transition from Versoyen-type Paleozoic basement and Mesozoic metasediments is indicated by the increasing matrix/clast ratio moving away from the contact with the Paleozoic basement (**a**, **b** and **c**); microfossils are locally preserved alongside metamorphic garnet and chloritoid in grey micaschists.

The excursion ends here. The main track connecting Tormottaz Lake with the car park can be reached walking downhill for a few tens of meters. Follow it southwards up to the Punta Rossa pass. Please note that the track, about 100 m to the north of the pass, ascends a relatively exposed cliff, which might be dangerous if snow is still accumulated at its base. In that case, backtracking is advised, following the main track to the north, walking up the slope to the left, then heading south until the NE-SW trending depression, which can now be followed to the E, until the Punta Rossa pass. Follow the main track downhill from there.

DOI: 10.3301/GFT.2014.01

LITHO-TECTONIC MAP OF THE LAGO DI CIGNANA AREA (UHP) AND ETIROL-LEVAZ SLIVER (VALTOURNENCHE, VALLE D'AOSTA, ITALY)

Compiled by D.Regis after: Regis, D. (2007), Manzotti, P. (2011), Forster et al. (2006), Groppo et al. (2009), Pleuger et al (2007).

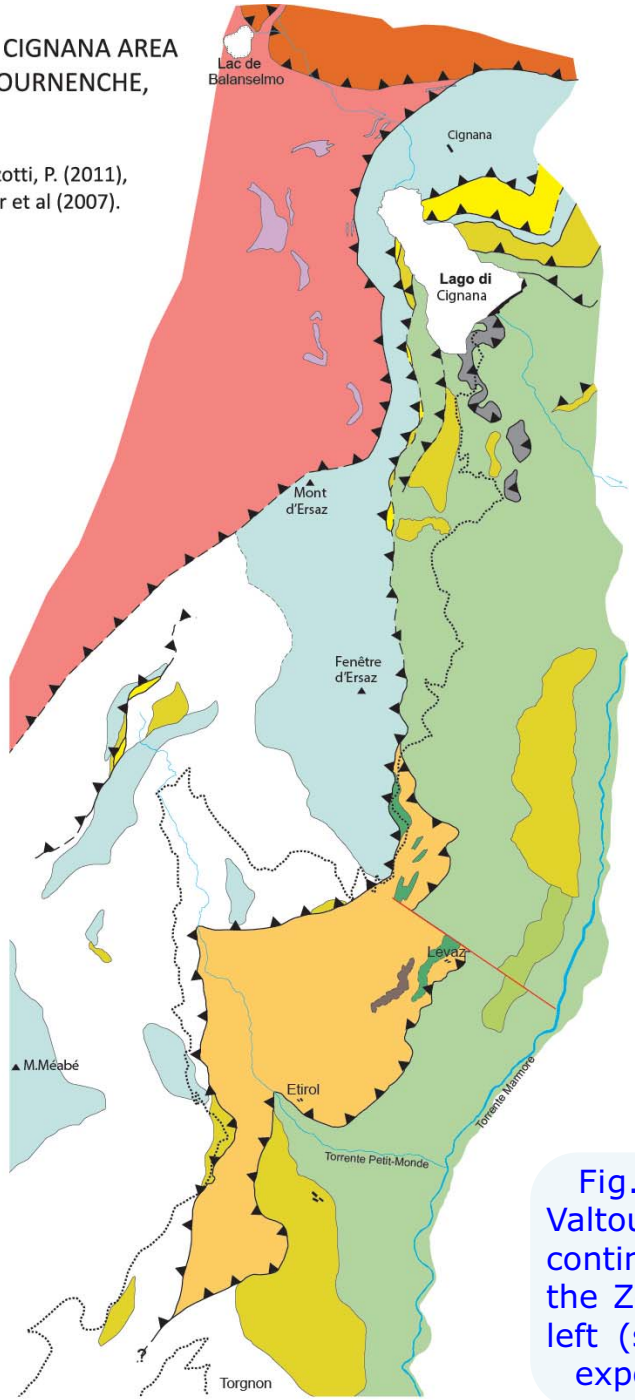

N

0 1km

Legend:

AUSTROALPINE UNIT

Valpelline Series
- HT metasediments and amphibolites

Arolla series
- Mesozoic metasediments (Roisan Zone)
- Permian metagranites and metaquartzodiorites

Etirol-Levaz slice
- Eclogitic micaschists s.l.
- Meta-gabbros
- Serpentinites and ultramafic rocks of Gilliarey

PIEMONTE UNIT

Combin Zone
- Calcschists and prasinites
- Serpentinites
- Triassic lithologies (Pancherot-Cime Bianche)

Zermatt-Saas Zone
- Eclogites
- UHP unit (Lago di Cignana)
- Meta-basalts and meta-gabbros
- Serpentinites

Main thrusts
Faults
Road

DAY2: Lago di Cignana unit, Zermatt-Saas zone, Valtournenche

Two main stops are scheduled: **Stop 2.1** is devoted to examine the meta-ophiolites of the Zermatt-Saas zone and of the Combin zone, and the continental crust of the Etirol-Levaz slice; the UHP unit of Lago di Cignana will be examined at **Stop 2.2**. Most of the road winds along the tectonic contact between the eclogite-facies Zermatt-Saas zone and the epidote-blueschist facies Combin zone, where the Etirol-Levaz continental crust slice is exposed (Fig. 18). The geometrical relationships among the different tectonic units are best seen from the opposite side of the valley (Fig. 25).

Fig. 18 – Lithotectonic map of the western side of Valtournenche from Torgnon to Lago di Cignana. The Etirol-Levaz continental crust slice occurs just at the tectonic contact between the Zermatt-Saas zone to the right and the Combin zone to the left (see also Fig. 3). The small UHP Lago di Cignana unit is exposed on the southern side of the lake.

DOI: 10.3301/GFT.2014.01

STOP 2.1 - Ophiolites of the Zermatt-Saas/Combin zone and Etirol-Levaz continental crust slice

Locality: Gilliarey (Dzilliarey) Chapel and surroundings. (Coord.: 7.586249 E; 45.841249 N, c. 2190 m a.s.l.)

The **Zermatt-Saas zone** consists mainly of antigorite serpentinite and eclogite. The serpentinite is composed of antigorite with relics of eclogite-facies clinopyroxene, olivine and Ti-clinohumite. The eclogite, derived from a Fe-Ti-gabbro protolith, consists of garnet and omphacite with minor glaucophane and phengite, and accessory rutile. Minor late-Alpine greenschist-facies overprint is indicated by albite, epidote, Ca-Na-amphibole and titanite.

The **Etirol-Levaz continental slice** is mainly composed of garnet-phengite micaschists and fine-grained phengite gneisses with layers and/or boudins of eclogite locally retrogressed to prasinite. A metagabbro has also been described from the core of this slice, on an almost inaccessible cliff (Kienast, 1983).

An orthogneiss sample collected at the bottom of the Etirol-Levaz slice just at the contact with the underlying Zermatt-Saas antigorite serpentinite has been the subject of high-precision *in-situ* geochronology (Beltrando et al., 2010a). The dated zircons show Permian magmatic cores overgrown by Jurassic (166-150 Ma) rims. This age, interpreted as due to the infiltration of melts associated to the intrusion of rift-related gabbroic magmas, indicates that the continental were already juxtaposed to the oceanic basement prior to the Alpine orogeny. The Alpine eclogite-facies overprint of the Etirol-Levaz continental slice, dated at 47.5±1.0 Ma (SHRIMP U/Pb zircon: Beltrando et al., 2010b), shows a prograde path peaking at 2.4 GPa and 550°C (Regis, 2007), which is overlapping the metamorphic history estimated for the Zermatt-Saas tectonic unit overlying the UHP Lago di Cignana unit (Groppo et al., 2009).

A small body of metaperidotite is exposed within the micaschists below the Gilliarey Chapel. Its origin is uncertain, as it may have been originally part of the continental slice or of the Zermatt-Saas zone. The peridotite hosts two generations of olivine (OlI = Fo_{87} and OlII = Fo_{92}) and Ti-clinohumite, relict Cr-spinel, and magnetite. Ti-clinohumite associated to OlI is replaced by ilmenite + antigorite, whereas Ti-clinohumite in equilibrium with OlII is fresh. The relict Cr-rich spinel (up to Cr_2O_3= 22 wt.%) is replaced by magnetite progressively depleted in Cr. Cr-free magnetite is included in OlII, suggesting the occurrence of a previous serpentinization process.

The **Combin zone** rocks are well exposed on the road cut a few tens of meters to the north of the Gilliarey Chapel. They mainly consist of the typical calcschist-prasinite association. Calcschist consist of cm-thick alternating white mica + chlorite layers and calcite-rich layers. Prasinite exhibits a typical greenschist-facies mineral assemblage actinolite + epidote + chlorite + poikiloblastic albite with abundant accessory titanite.

DOI: 10.3301/GFT.2014.01

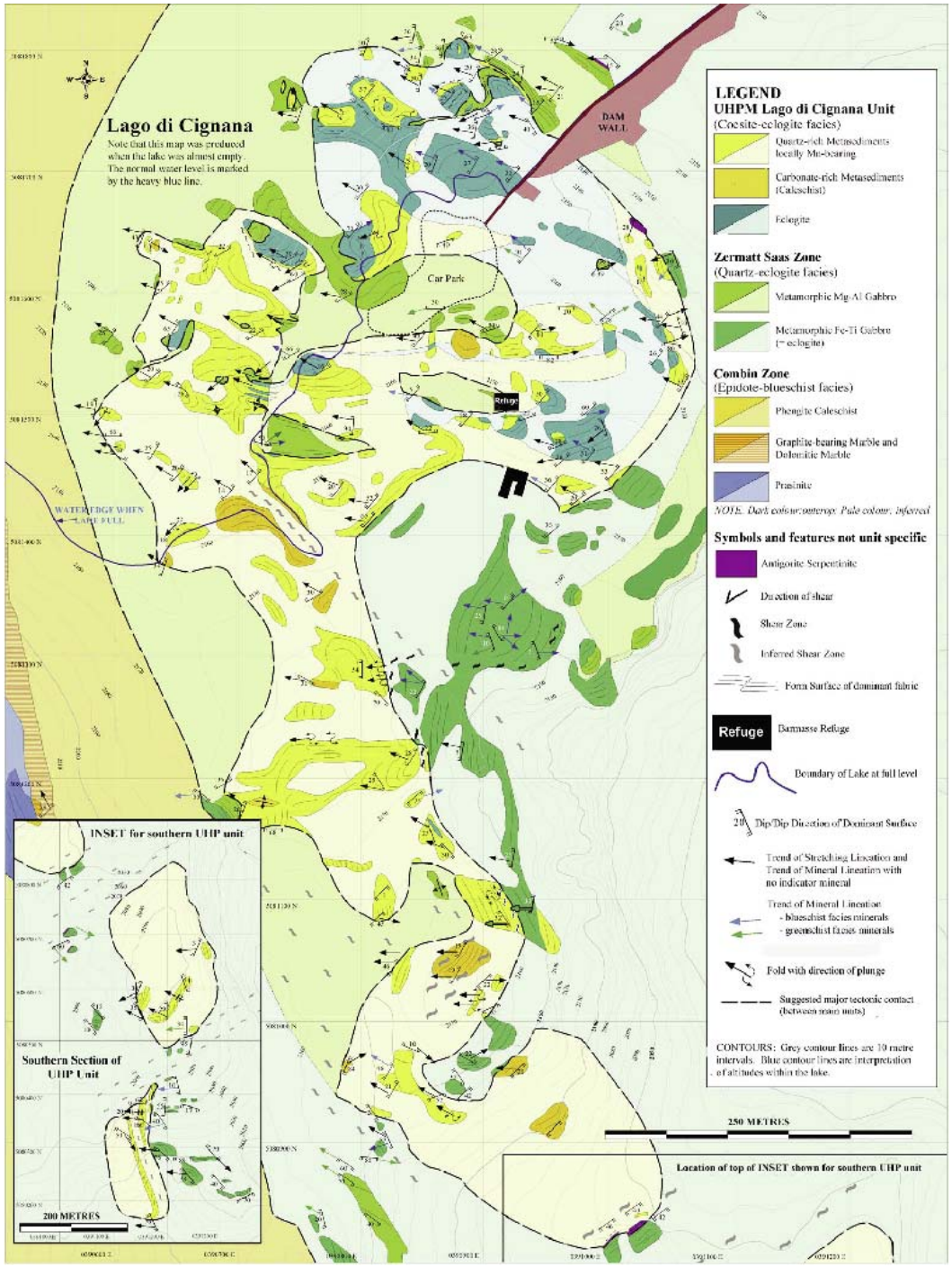

STOP 2.2 - The UHP Lago di Cignana unit (LCU)

The minivans will stop at the parking place close to the southern end of the Lago di Cignana dam. (Coord.: 7.593070 E; 45.877972 N, c. 2165 m a.s.l.)

Stop 2.2a: Eclogites exposed to the south of the lake shore close to the dam

The best outcrop of the LCU eclogites, polished by the Quaternary glacier, is here exposed. The local presence of narrow glaucophane-garnet layers and streaks wrapping around metre-sized eclogite layers and pods has been interpreted by Reinecke et al. (1994) as evidence of original pillow structures. Major, minor and trace elements indicate that the eclogites derive from a mid-ocean ridge tholeiitic protolith (Groppo et al., 2009).

The eclogites are medium grained foliated and locally lineated rocks with characteristic mm-sized yellowish lozenge-shaped aggregates after former porphyroblastic lawsonite. The UHP peak

Fig. 19 – Geologic map of the UHP Lago di Cignana unit (from Forster et al., 2004). The schistosity shown on the map is the main regional schistosity associated with boudin formation. Relict older fabrics and overprinting younger fabrics occur throughout the UHP unit. Various deformational events have occurred, in particular several different stages of shear zones.

DOI: 10.3301/GFT.2014.01

assemblage consisted of omphacite + garnet + glaucophane + lawsonite (now epidote + paragonite ± phengite pseudomorphs) + minor phengite and accessory rutile. The matrix foliation (S_m) is mainly defined by the alignment of elongated omphacite crystals and curves around porphyroblastic garnet up to 5 mm in diameter (Groppo et al., 2009). A complex growth history can be inferred for garnet porphyroblasts on the basis of their strong compositional zoning and inclusion distribution (Groppo et al., 2009). Three main zones have been recognized (Fig. 26a): **i)** a garnet core crowded with very small inclusions of omphacite, Ca-amphibole, epidote, ilmenite and very rare biotite, locally defining an internal foliation (S_{m-1}); **ii)** a garnet mantle characterized by coarser-grained, randomly oriented inclusions, concentrated at the core–mantle interface, of NaCa-amphibole, omphacite, quartz, rutile and lozenge-shaped epidote + paragonite ± phengite aggregates after former lawsonite; **iii)** a garnet rim, very thin (50–100 μm) compared to the garnet core and mantle, free of inclusions. The eclogites display a variable degree of greenschist-facies retrogression, the most intense occurring along straight fractures, where the infiltration of a hydrous fluid phase has produced a typical "prasinitic" (Ab+Chl+Act+Ep) assemblage, with local enrichment of porphyroblastic albite. The whole prograde, peak and retrograde eclogite evolution is summarized in the diagram of Fig. 20.

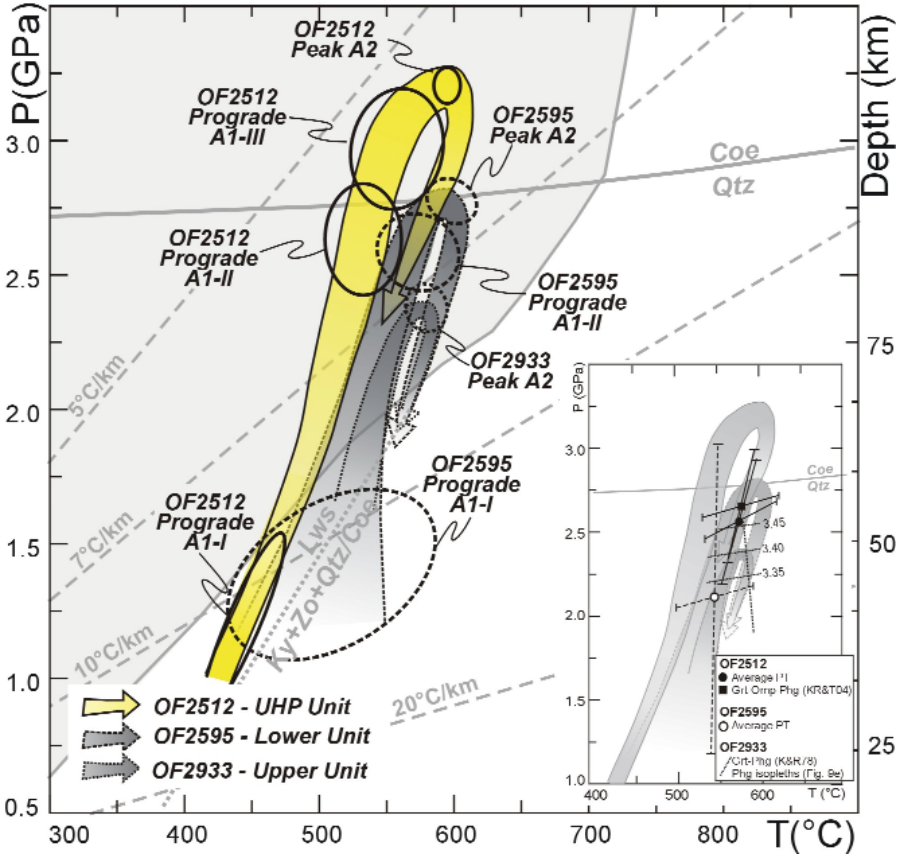

Fig. 20 – *P-T* path of the UHP LCU and adjoining units (from Groppo et al., 2009, Fig. 12). The evolution of the LCU, highlighted in yellow, was inferred from the eclogite sample OF2512. Continuous ellipses show prograde (A1-I, A1-II and A1-III), and peak (A2) conditions for eclogite OF2512, as derived from the compositional isopleths modelled in the pseudosections (Figs. 10 and 11 in Groppo et al., 2009). The lawsonite stability field, as inferred from the same pseudosections, is reported in pale grey. The Lws = Ky + Zo + Qtz / Coe reaction is from Poli & Schmidt (1998). In the inset, the P–T constraints derived from conventional thermobarometry and Average PT method (Powell & Holland, 1988) are reported and compared with the P–T paths reconstructed on the base of pseudosection analysis. Numbers in italics refer to the Si(Phg) isopleths modelled for eclogite OF2512 (LCU) (Fig. 10e in Groppo et al., 2009).

DOI: 10.3301/GFT.2014.01

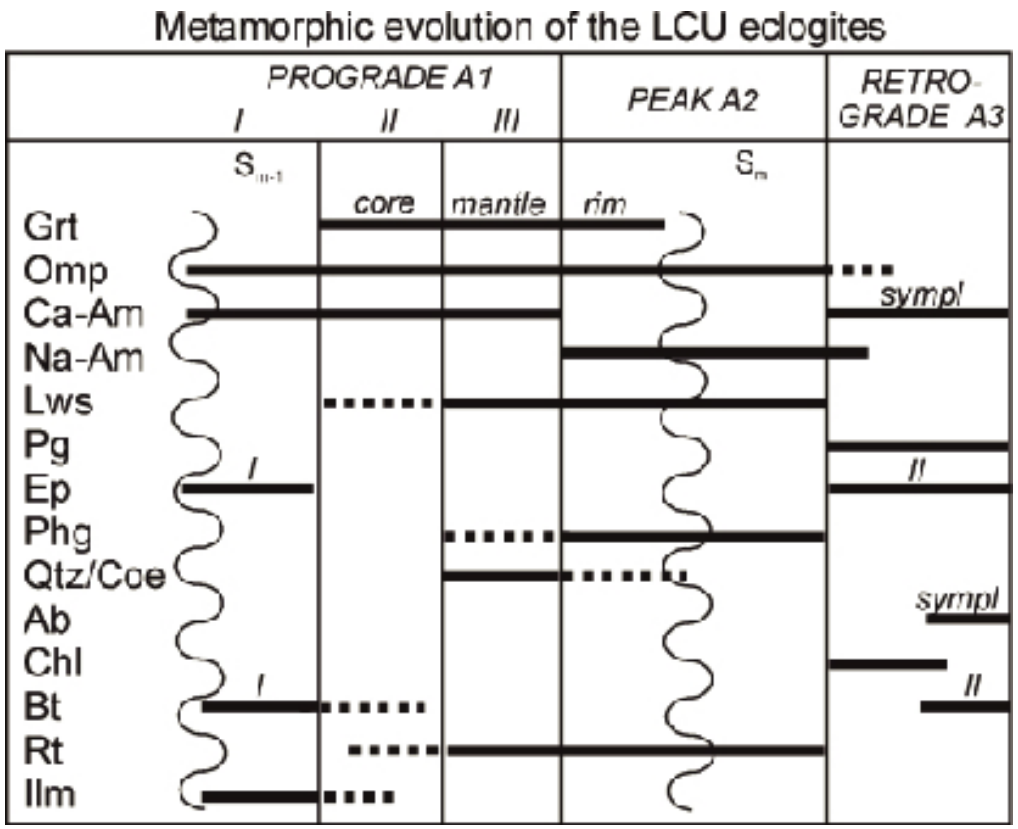

Fig. 21 – Metamorphic evolution of the LCU eclogites (from Groppo et al., 2009). Sm= matrix foliation; Sm-1 = relict foliation, earlier than Sm, preserved in microlithons or as internal foliation (Si) in garnet porphyroblasts. Symp: green-amphibole + albite symplectite.

Stop 2.2b: Metasedimentary siliceous and carbonate rocks exposed along the lake shore

As described before, the LCU metasedimentary cover consists of glaucophane-garnet-ex-lawsonite quartz-phengite-carbonate schists with dm-thick intercalations of yellowish quartz-phengite-garnet marbles, and nodules or boudinaged layers of garnetite (Tamagno, 2000). The quartz-mica-carbonate schist grades to impure quartzite and quartz-rich micaschist with phengite, garnet, glaucophane, ± omphacite, ± ex-lawsonite, ± chloritoid. Accessory minerals are apatite, rutile, green to light brown tourmaline, elongated opaque ores, and zircon.

Where quartz-rich micaschist and quartzite are Mn-bearing, new minerals appear such as piemontite, clinozoisite/epidote, Mn-bearing phengite, Mn-rich garnet and black nodules. These nodules, up to a few cm across, consist of a core composed of braunite + yellowish–greenish garnet and carbonates, and a rim composed of an aggregate of clear garnet with oriented inclusions of elongated opaque ores, haematite, piemontite and/or epidote, local quartz, and pseudomorphs after former Na-rich clinopyroxene. These pseudomorphs are also common in the micaschist matrix. Black nodules have a spongy appearance for selective dissolution of carbonates. At least two different phengite generations, locally and pinkish in colour (Mn-bearing), are observed: an older coarser-grained celadonitic richer and a younger finer-grained celadonitic poorer.

DOI: 10.3301/GFT.2014.01

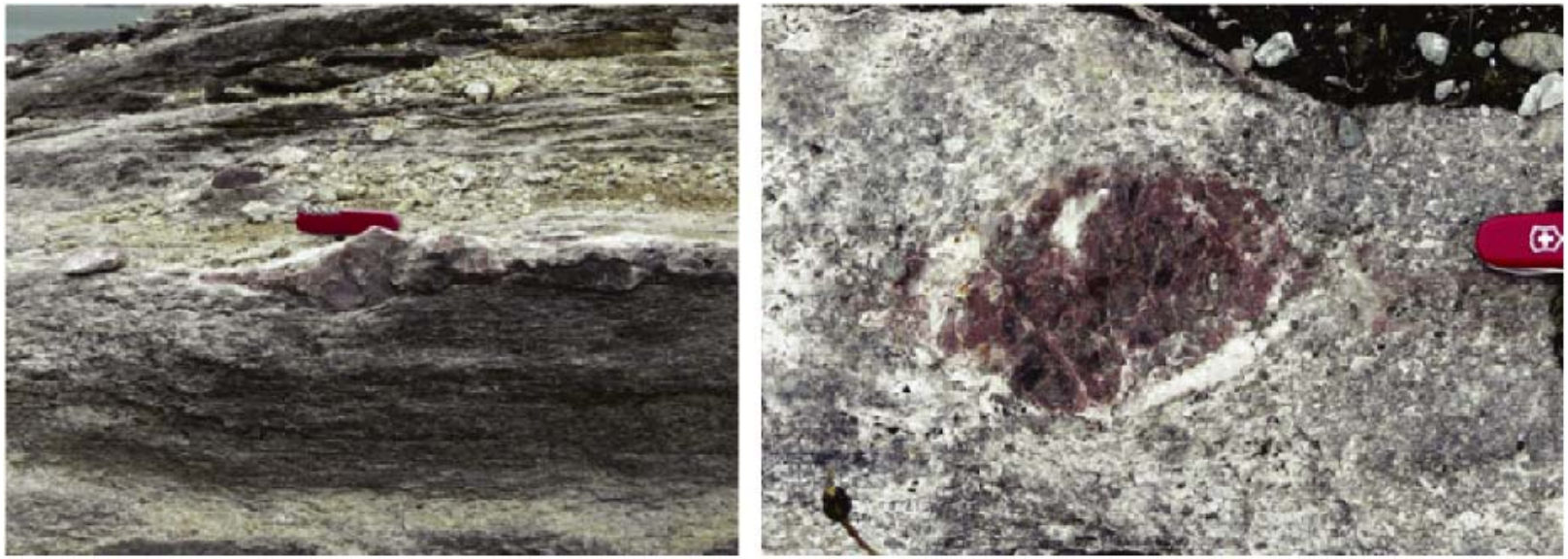

Fig. 22 – Boudinaged Mn-garnetite layer (left) and nodule (right) occurring in quartz-rich phengite micaschist or in impure quartzite.

In a detailed study of Mn-bearing quartz-rich schists and quartzites, Reinecke (1998) distinguished talc-garnet-phengite-piemontite quartz-rich schists and Na-clinopyroxene-epidote-phengite-garnet quartzites. Al-rich portions consist of the peak UHP assemblage: Mn-rich garnet + coesite + Mn-phlogopite + kyanite + haematite + rutile + piemontite + zircon, whereas the Al-poor portions consist of garnet + coesite + phlogopite + talc + phengite + piemontite + haematite + rutile + braunite + ardennite + dravite + apatite + paragonite + zircon. The above lithologies may contain rare boudins of garnetite, omphacitite and jadeitite. As to the garnetite description, see above.

DOI: 10.3301/GFT.2014.01

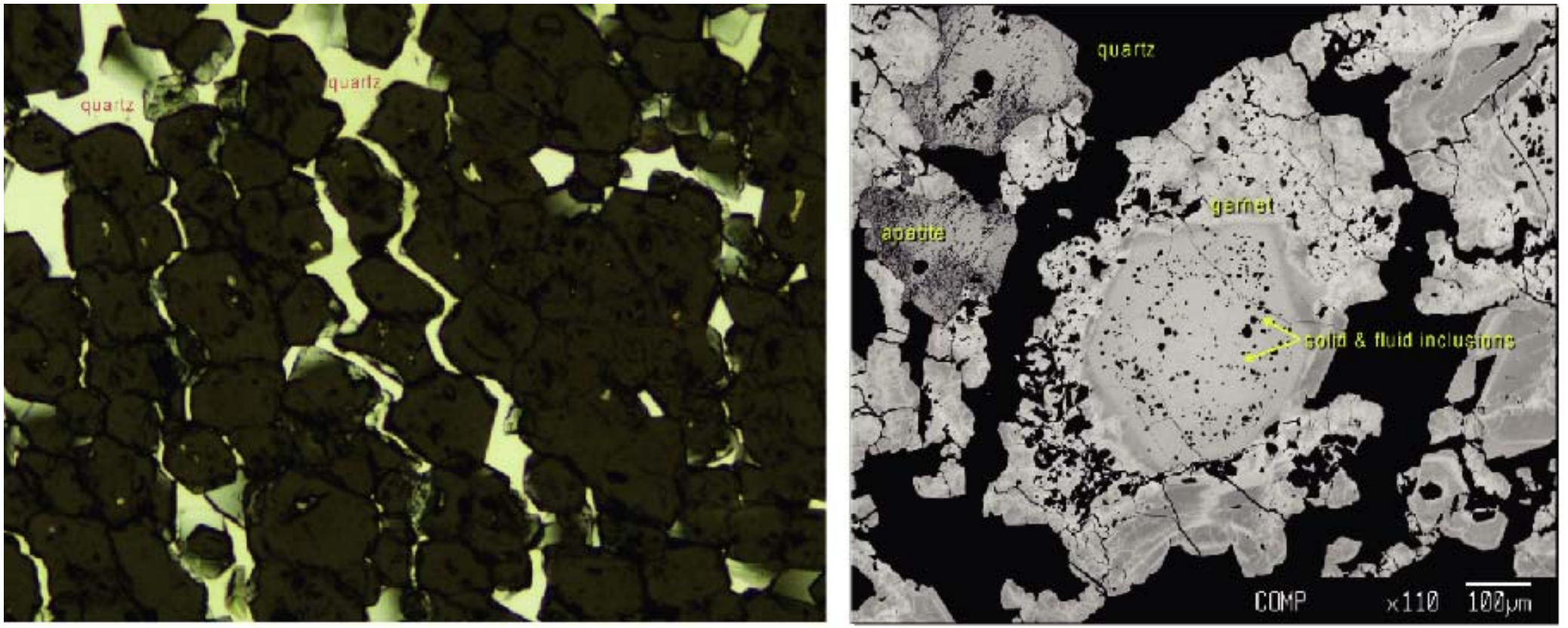

Fig. 23 – Left: Microphotograph of the margin of a garnetite nodule, where massive garnetite is dismembered and fragments are included in cm-sized quartz poikiloblasts. Right: BSE image that shows the garnet zoning with solid and fluid inclusions in the core and quartz inclusions in the late overgrowth. Note the accessory apatite dusty for very fine-grained solid inclusions.

During the pervasive greenschist-facies retrogression the UHPM minerals have been pseudomorphically replaced by aggregates of new lower-*P* minerals: blue amphibole by albite + chlorite, omphacite by albite + magnetite + haematite ± white mica ± green amphibole, jadeite by a felt of tiny oriented green amphibole needles ± opaque ores ± haematite in a matrix of fine grained albite, lawsonite by clinozoisite + paragonite, garnet by earlier biotite and later chlorite, phengite by albite ± earlier green-brown biotite ± later chlorite. The alteration of phengite to albite, which is a metasomatic process widespread in the basement rocks of the Western Alps, converts the phengite micaschist to albite gneiss.

DOI: 10.3301/GFT.2014.01

Stop 2.2c: Thin layers of sheared metagabbro with fuchsite pseudomorphs after original Cr-clinopyroxene at the upper contact with the Zermatt-Saas Zone

The tectonic contact between metasediments of the UHP LCU and the HP Zermatt-Saas Zone is evident in several sites along the lake shore, where the exposure is continuous. The contact is marked by a thin skin of highly deformed metagabbro from the Zermatt-Saas Zone. However, in spite of the Alpine polyphase tectono-metamorphic overprint, in the lowest strain zones relics of the original coarse grained igneous structure is still evident for preservation of cm-sized bright green pseudomorphs after the igneous Cr-bearing clinopyroxene, which is now consisting of a fuchsite aggregate.

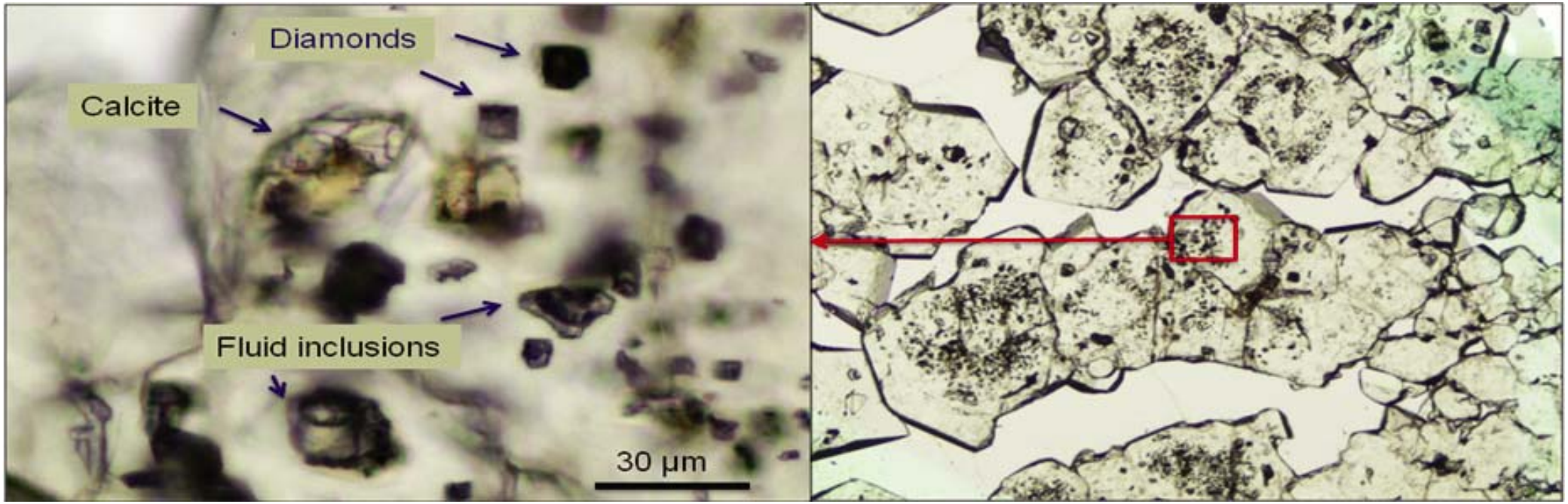

Fig. 24 – Distribution of diamonds and other inclusions in garnet cores.

DOI: 10.3301/GFT.2014.01

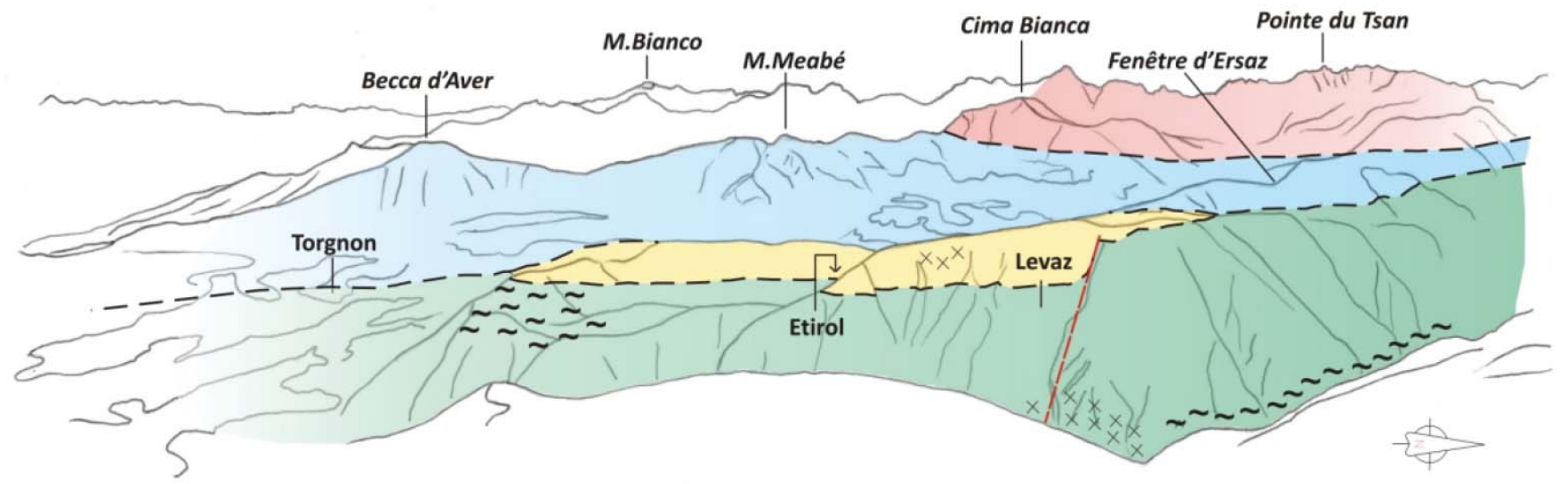

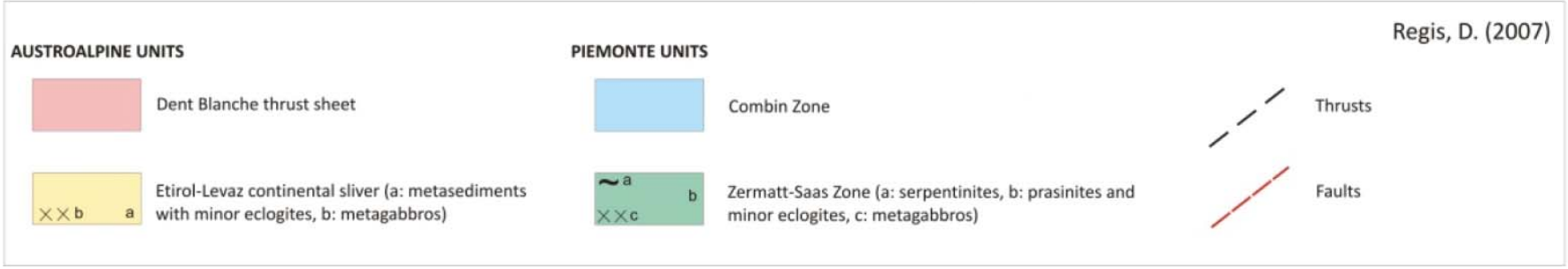

Fig. 25 – Panoramic view **(a)** and a simplified geotectonic sketch **(b)** of the right side of the middle Valtournenche between Torgnon (left) and Lago di Cignana (right). The Etirol-Levaz continental crust (pale yellow) is sandwiched between the underlying eclogite-facies Zermatt-Saas zone (green) and the overlaying epidote blueschist-facies Combin zone (light blue), which is cupped by the Austroalpine Dent Blanche nappe (reddish).

DOI: 10.3301/GFT.2014.01

Fig. 26 – Representative microstructures of LCU eclogites as seen under optical microscope and SEM (Fig. 3 in Groppo et al., 2009). **(a)** Strongly zoned porphyroblastic garnet (Grt) set in an omphacite (Omp) + glaucophane (Gln) matrix. In garnet, three main zones are evident: a core, characterized by an internal foliation (S_{m-1}) mainly defined by very fine-grained inclusions of omphacite + amphibole; a mantle, with coarser-grained randomly oriented inclusions of omphacite, amphibole (Am), former lawsonite, quartz (Qtz) and rutile (Rt); a very thin, inclusion-free rim. Garnet is partially replaced by biotite (Bt). Plane Polarized Light (PPL). **(b)** Coarse-grained glaucophane (Gln) in the matrix, partially replaced by a symplectite of Ca-amphibole + albite (Sympl) (PPL). **(c)** Glaucophane (Gln) rimmed with green-blue NaCa-amphibole (Am) and a phengite (Phg) flake in the matrix (PPL).

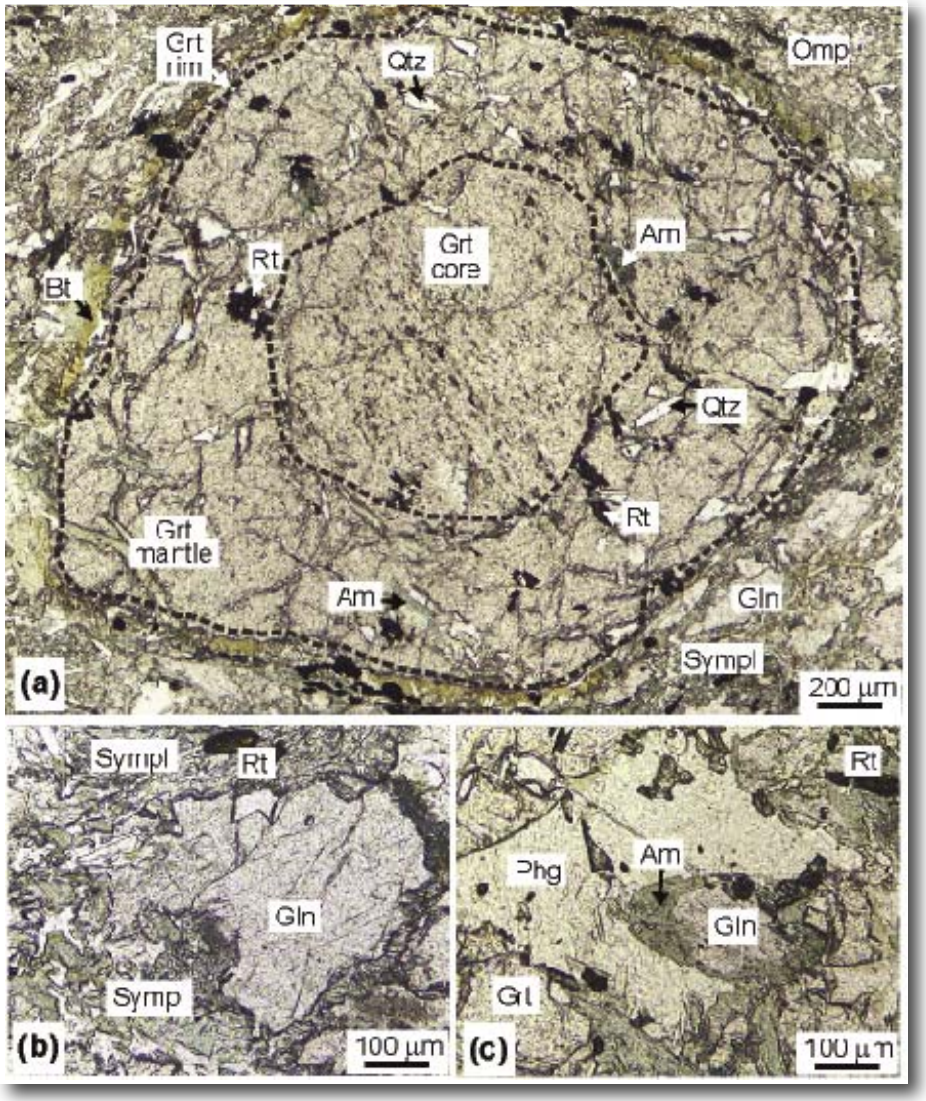

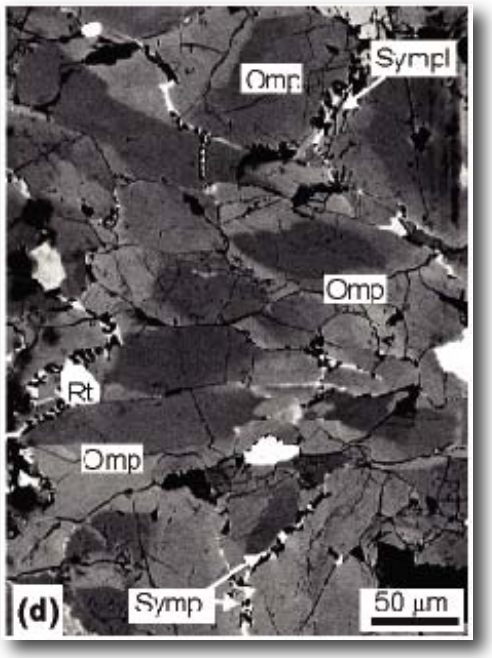

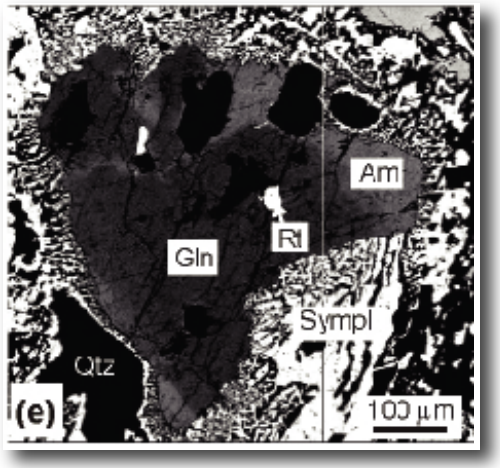

(d) Back-Scattered Electron (BSE) image of zoned omphacite (Omp) from the matrix. **(e)** BSE image of a zoned glaucophane (Gln) rimmed with blue–green amphibole (Am) and partially replaced by a green amphibole + albite symplectite (Sympl). Rutile (Rt) inclusions occur in the glaucophane core. The whole inferred metamorphic evolution is summarized in Fig. 21.

DOI: 10.3301/GFT.2014.01

DOI: 10.3301/GFT.2014.01

References

Agard P., Yamato P., Jolivet L. & Burov E. (2009) - Exhumation of oceanic blueschists and eclogites in subduction zones: timing and mechanisms. Earth Sci. Rev., 92, 53–79.

Amato J.M., Johnson C.M., Baumgartner L.P. & Beard B.L. (1999) - Rapid exhumation of the Zermatt-Saas ophiolite deduced from high-precision Sm-Nd and Rb-Sr geochronology. Earth and Planetary Science Letters, 171, 425–438.

Angiboust S., Agard P., Jolivet L. & Beyssac O. (2009) - The Zermatt-Saas ophiolite: the largest (60-km wide) and deepest (c. 70–80 km) continuous slice of oceanic lithosphere detached from a subduction zone? Terra Nova, 21, 171–180.

Antoine P. (1965) - Sur l'existence du Crétacé supérieur daté dans la nappe des Brèches de Tarentaise au Nord des Chapieux (Savoie). Comptes Rendus de l'Académie de Sciences de Paris 261, 3640-3642.

Antoine P. (1971) - La Zone des Brèches de Tarentaise entre Bourg-St-Maurice (Vallée d'Isère) et la frontière italo-suisse. Travaux du Laboratoire Géologie de l'Université de Grenoble, Mémoires 9, 1-367.

Baijot M., Hatert F. & Fransolet A.-M. (2011) - Mineralogical and geochemical study of pseudocoticule from the Stavelot Massif, Ardennes (Belgium), and redefinition of coticule. Eur. J. Mineral., 23, 633–644.

Bearth P. (1967) - Die Ophiolithe der Zone von Zermatt-Saas Fee. Beiträge zur geologischen Karte der Schweitz, Neue Folge, 132, 1-130.

Beltrando M., Compagnoni R. & Lombardo B. (2010a) - (Ultra-) High-pressure metamorphism and orogenesis: An Alpine perspective, Gondwana Research 18, 147-166, doi:10.1016/j.gr.2010.01.009

Beltrando M., Frasca, G., Compagnoni, R. & Vitale Brovarone A. (2012) - The Valaisan controversy revisited: multi-stage folding of a Mesozoic hyper-extended margin in the Petit St. Bernard pass area (Western Alps). Tectonophysics, 579, 17-36, doi: 10.1016/j.tecto.2012.02.010

Beltrando M., Manatschal G., Mohn G., Dal Piaz G.V., Vitale Brovarone A. & Masini E. (2014) - Recognizing remnants of magma-poor rifted margins in high-pressure orogenic belts: The alpine case study. Earth Science Reviews, doi: 10.1016/j.earscirev.2014.01.001

Beltrando M., Rubatto D., Compagnoni R. & Lister G. (2007) - Was the Valaisan basin floored by oceanic crust? Evidence of Permian magmatism in the Versoyen Unit (Valaisan domain, NW Alps). Ofioliti, 32, 85-99.

Beltrando M., Rubatto D. & Manatschal G. (2010b) - From passive margins to orogens: The link between Ocean-Continent Transition zones and (Ultra-)High-Pressure metamorphism. Geology, 38(6), 559-562, doi:10.1130/G30768.1

Beltrando M., Zibra I., Montanini A. & Tribuzio R. (2013) - Crustal thinning and exhumation along a fossil magma-poor distal margin preserved in Corsica: A hot rift to drift transition? Lithos, 168-169, 99–112, doi: 10.1016/j.lithos.2013.01.017

Bigi G., Castellarin A., Coli M., Dal Piaz G.V., Sartori R., Scandone P. & Vai G.B. (1990) - Structural model of Italy 1:500.000, sheet 1. C.N.R., Progetto Finalizzato Geodinamica, S.E.L.CA., Firenze.

Bousquet R., Goffé B., Vidal O., Oberhänsli R. & Patriat M. (2002) - The tectono-metamorphic history of the Valaisan domain from the Western to the Central Alps: New constraints on the evolution of the Alps. Geol. Soc. Am. Bull., 114, 207-225.

DOI: 10.3301/GFT.2014.01

Burri M. (1979) - Les formations valaisannes dans la région de Visp. Eclogae geologicae Helvetiae, 72, 789–802.
Cannic S. (1996) - L'évolution magmatique et tectono-métamorphique du substratum du Domain Valaisan (complexe du Versoyen, Alpes Occidentales): implications dans l'histoire alpine. PhD. Thesis, Université de Grenoble, 142 p.
Cannic S., Mugnier J.L. & Lardeaux J.M. (1995) - Mise en évidence d'une faille normale ductile dans l'unité du Roignais-Versoyen. Comptes Rendus de l'Académie des Sciences, Paris, 321, 513-519.
Cannic S., Lardeux J.M., Mugnier J.L. & Hernandez J. (1996) - Tectono-metamorphic evolution of the Roignais-Versoyen Unit (Valaisan domain, France). Eclogae geologicae Helvetiae, 89, 321-343.
Dal Piaz G.V. (1974) - Le métamorphisme de haute pression et basse température dans l'évolution structurale du bassin ophiolitique alpino-apenninique. Schweizerische mineralogische und petrographische Mitteilungen, 54, 399–424.
Dal Piaz G.V., Di Battistini G., Kienart J.-R. & Venturelli G. (1979) - Manganiferous quartzitic schists of the Piemonte ophiolite nappe in the Valsesia-Valtournanche area (Italian Western Alps). Memorie di Scienze Geologiche, Padova, 32, 1-24.
Dal Piaz G.V. (1999) - The Austroalpine–Piedmont nappe stack and the puzzle of Alpine Tethys. Memorie di Scienze Geologiche, Padova, 51, 155–176.
Day H.W. (2012) - A revised diamond-graphite transition curve. American Mineralogist, 97, 52–62.
Decandia F.A. & Elter P. (1972) - La zona ofiolitifera del Bracco nel settore compreso tra Levanto e la Val Graveglia (Appennino Ligure). Memorie Società Geologica Italiana, 11, 503–530.
Dewey J.F., Helma M.L., Turco E., Hutton D.H.W. & Knott S.D. (1989) - Kinematics of the western Mediterranean. In: M.P. Coward, D. Dietrich, R.G. Park (Eds.). Alpine Tectonics, Geological Society Special Publication, 45, 265–283.
Durand-Delga M., Peybernès B. & Rossi P. (1997) - Arguments en faveur de la position, au Jurassique, des ophiolites de Balagne (Haute-Corse, France) au voisinage de la marge continentale européenne. Comptes Rendus de l'Académie des Sciences, Paris 325, 973–998.
Elter P. (1954) - Etudes géologiques dans le Val Veny et le Vallon du Breuil (Petit St. Bernard). Thèse, Univ. Genève, 1-38.
Elter G. & Elter P. (1957) - Sull'esistenza, nei dintorni del Piccolo S. Bernardo, di un elemento tettonico riferibile al ricoprimento del Pas du Roc. Rendiconti Accademia Nazionale dei Lincei, 22, 181-187.
Elter G. & Elter P. (1965) - Carta geologica della regione del Piccolo San Bernardo (versante italiano). Note illustrative. Memorie dell'Istituto di Geologia e Mineralogia dell'Università di Padova 25, 1-53.
Escher A., Hunziker J.C., Marthaler M., Masson H., Sartori M. & Steck A. (1997) - Geologic framework and structural evolution of the Western Swiss-Italian Alps. In: Pfiffner O., Lehner P., Heitzmann P., Mueller S. & Steck A. (Eds.). Results of NRP 20, Deep structures of the Swiss Alps, Birkhäuser, 205-221.
Florineth D. & Froitzheim N. (1994) - Transition from continental to oceanic basement in the Tasna nappe (Engadine window, Graubünden, Switzerland): Evidence for Early Cretaceous opening of the Valais ocean. Schweizerische mineralogische und petrographische Mitteilungen, 74, 437-448.
Forster M., Lister G., Compagnoni R., Giles D., Hills Q., Betts P., Beltrando M. & Tamagno E. (2004) - Mapping of oceanic crust with "HP" to "UHP" metamorphism: The Lago di Cignana Unit (Western Alps). In: G. Pasquarè, C. Venturini (Eds.), G. Groppelli (Ass. Ed.) Mapping Geology in Italy, APAT- Dipartimento Difesa del Suolo – Servizio Geologico d'Italia, Roma (2006), Map 33, 279-286, Printed by S.EL.CA. - Firenze.

DOI: 10.3301/GFT.2014.01

Franchi S. (1899) - Nuove località con fossili mesozoici nella zona delle pietre verdi presso il colle del Piccolo San Bernardo (Valle d'Aosta). Bollettino Comitato Geologico Italiano, 10, 303-324.

Frezzotti M.L., Selverstone J., Sharp Z.D. & Compagnoni R. (2011) - Carbonate dissolution during subduction revealed by diamond-bearing rocks from the Alps. Nature Geoscience, 4/10, 703-706.

Fried L.E. & Howard W.M. (2000) - Explicit Gibbs free energy equation of state applied to the carbon phase diagram. Physical Review B: Condensed Matter, 61, 8734–8743.

Froitzheim N. & Eberli G.P. (1990) - Extensional detachment faulting in the evolution of a Tethys passive continental margin, Eastern Alps, Switzerland, Geol. Soc. Am. Bull., 102, 1297–1308.

Froitzheim N. & Manatschal G. (1996) - Kinematics of Jurassic rifting, mantle exhumation, and passive-margin formation in the Austroalpine and Penninic nappes (Eastern Switzerland). Geol. Soc. Am. Bull., 108, 1120-1133.

Fügenschuh B., Loprieno A., Ceriani S. & Schmid S.M. (1999) - Structural analysis of the Subbriançonnais and Valais units in the area of Moûtiers (Savoy, Western Alps): paleogeographic and tectonic consequences. International Journal of Earth Sciences, 88, 201-218.

Gerya T., Stöckhert B. & Perchuk A.L. (2002) - Exhumation of high pressure metamorphic rocks in a subduction channel-a numerical simulation. Tectonics, 21, 1–19.

Goffé B. & Bousquet R. (1997) - Ferrocarpholite, chloritoid and lawsonite in metapelites of the Versoyen and Petit St. Bernard units (Valais zone, Western Alps). Schweizerische mineralogische und petrographische Mitteilungen, 77, 137-147.

Gouzu C., Itaya T., Hyodo H. & Matsuda T. (2006) - Excess ^{40}Ar-free phengite in ultrahigh-pressure metamorphic rocks from the Lago di Cignana area, Western Alps. Lithos, 92, 418–430.

Groppo C., Beltrando M. & Compagnoni R. (2009) - P-T path of the UHP Lago di Cignana and adjoining HP meta-ophiolitic units: insights into the evolution of the subducting Tethyan slab. Journal of Metamorphic Geology, 27, 207–231.

Hermann F. (1930) - Studi geologici nelle Alpi Occidentali- La regione del Piccolo San Bernardo. Memorie Istituto di Geologia Università di Padova, 8, 72-80.

Kelts K. (1981) - A comparison of some aspects of sedimentation and translational tectonics from the Gulf of California and the mesozoic Tethys. Eclogae geologicae Helvetiae, 74, 317-338.

Kennedy C.S. & Kennedy G.C. (1976) - The equilibrium boundary between graphite and diamond. Journal of Geophysical Research, 81, 2467-2470.

Kienast J.R. (1983) - Le métamorphisme de haute pression et basse température (Eclogites et Schistes Blues): données nouvelles sur la pétrologie de la croûte océanique subductée et des sédiments associés. Unpublished Thèse d'Etat Thesis, Université de Paris VI, Paris.

King R.L., Bebout G.E., Kobayashi K., Nakamura E. & van der Klauw S.N.G.C. (2004) - Ultrahigh-pressure metabasaltic garnets as probes into deep subduction zone chemical cycling. Geochemistry Geophysics Geosystems, 5, Q12J14.

Krogh E. J. & Råheim A. (1978) - Temperature and pressure dependence of Fe-Mg partitioning between garnet and phengite, with particular reference to eclogites. Contributions to Mineralogy and Petrology, 66, 75–80.

Krogh Ravna E. J. & Terry M.P. (2004) - Geothermobarometry of UHP and HP eclogites and schists – an evaluation of equilibria among garnet-clinopyroxene-kyanite-phengite-coesite/quartz. Journal of Metamorphic Geology, 22, 579–592.

DOI: 10.3301/GFT.2014.01

Lamens J., Geukens F. & Viane W. (1986) - Geological setting and genesis of coticules (spessartine metapelites) in the Lower Ordovician of the Stavelot Massif, Belgium. Journal of Geological Society London, 143, 253–258.

Lanari P., Guillot S., Schwartz S., Vidal O., Tricart P., Riel N. & Beyssac O. (2012) - Diachronous evolution of the alpine continental subduction wedge: Evidence from P–T estimates in the Briançonnais Zone houillère (France – Western Alps). Journal of Geodynamics, 56–57, 39–54.

Lapen T.J., Johnson C.M., Baumgartner L.P., Mahlen N.J., Beard B.L. & Amato J.M. (2003) - Burial rates during prograde metamorphism of an ultra-high-pressure terrane: an example from Lago di Cignana, Western Alps, Italy. Earth and Planetary Science Letters, 215, 57–72.

Lemoine M. (1985) - Structuration jurassique des Alpes occidentals et palinspastique de la Téthys ligure. Bull. Soc. Géol. Fr., 8, 126–137.

Lister G.S. & Forster M. (2009) - Tectonic mode switches and the nature of orogenesis. Lithos, 113, 274–291.

Lombardo B., Rubatto D. & Castelli D. (2002) - Ion microprobe U-Pb dating of zircon from a Monviso metaplagiogranite: implications for the evolution of the Piedmont-Liguria Tethys in the Western Alps. Ofioliti, 27, 109–117.

Loprieno A., Bousquet R., Bucher S., Ceriani S., Dalla Torre F.H., Fügenschuh B. & Schmid S.M. (2011) - The Valais units in Savoy (France): a key area for understanding the palaeogeography and the tectonic evolution of the Western Alps. International Journal of Earth Sciences, 100, 963–992.

Loubat H. (1968) - Étude pétrographique des ophiolites de la «zone du Versoyen», Savoie (France), Province d'Aoste (Italie). Archives des Sciences de la Société de Physique et d'Histoire Naturelle de Genève, 2, 265-457.

Loubat H. (1975) - La zone du Versoyen: témoin possible d'une intersection entre dorsale océanique et marge continentale. Archive des Sciences, Genève, 28, 101-116.

Manatschal G. (2004) - New models for evolution of magma-poor rifted margins based on a review of data and concepts from West Iberia and the Alps. Int. J. Earth Sci. (Geol. Rundsch.), 93, 432–466.

Manatschal G. & Nievergelt P. (1997) - A continent-ocean transition recorded in the Err and Platta nappes (Eastern Switzerland), Eclogae geologicae Helvetiae, 90, 3–27.

Manatschal G., Engström A., Desmurs L., Schaltegger U., Cosca M., Müntener O. & Bernoulli D. (2006) - What is the tectono-metamorphic evolution of continental break-up: the example of the Tasna Ocean-Continent Transition. Journal of Structural Geology, 28, 1849-1869.

Manatschal M. & Müntener O. (2009) - A type sequence across an ancient magma-poor ocean–continent transition: the example of the western Alpine Tethys ophiolites. Tectonophysics, 473, 4–19.

Marroni M., Molli G., Montanini A. & Tribuzio R. (1998) - The association of continental crust rocks with ophiolites (Northern Apennine, Italy): implications for the continent-ocean transition. Tectonophysics, 292, 43–66.

Masini E., Manatschal G., Mohn G., Ghienne J.F. & Lafont F. (2011) - The tectono-sedimentary evolution of a supra-detachment rift basin at a deep-water magma-poor rifted margin: The example of the Samedan Basin preserved in the Err nappe in SE Switzerland. Basin Res., 23, 652–677.

Masini E., Manatschal G. & Mohn G. (2013) - The Alpine Tethys rifted margins: reconciling old and new ideas to understand the stratigraphic architecture of magma-poor rifted margins. Sedimentology, 60, 174-196.

DOI: 10.3301/GFT.2014.01

Masson H., Bussy F., Eichenberger M., Giroud N., Meilhac C. & Preisniakov S. (2008) - Early Carboniferous age of the Versoyen ophiolites and consequences: non-existence of a "Valais ocean" (Lower Penninic, Western Alps). Bulletin de la Société Géologique de France, 4, 337-355.

Meresse F., Lagabrielle Y., Malavieille J. & Ildefonse B. (2012) - A fossil Ocean–Continent Transition of the Mesozoic Tethys preserved in the Schistes Lustrés nappe of northern Corsica. Tectonophysics, 579, 4-16, doi:10.1016/j.tecto.2012.06.013

Mohn G., Manatschal G., Muntener O., Beltrando M. & Masini E. (2010) - Unravelling the interaction between tectonic and sedimentary processes during lithospheric thinning in the Alpine Tethys margins. International Journal of Earth Sciences, 99, 75-101, doi: 10.1007/s00531-010-0566-6

Mohn G., Manatschal G., Beltrando M., Masini E. & Kusznir N. (2012) - Necking of continental crust in magma-poor rifted margins: Evidence from the fossil Alpine Tethys margins. Tectonics, 31, TC1012, doi: 10.1029/2011TC002961

Molli G. (1996) - Pre-orogenic tectonic framework of the northern Apennine ophiolites. Eclogae geologicae Helvetiae, 89, 163–180.

Mugnier J.L., Cannic S. & Lapierre H. (2008) - The tholeiites of the Valaisan domain (Versoyen, Western Alps): a Carboniferous magma emplaced in a small oceanic basin. Bulletin de la Société Géologique de France, 179, 357-368.

Péron-Pinvidic G. & Manatschal G. (2009) - The final rifting evolution at deep magma-poor passive margins from Iberia-Newfoundland: a new point of view. International Journal of Earth Sciences, 98, 1581–1597, doi: 10.1007/s00531-008-0337-9

Perotto A., Salino C., Pognante U., Genovese G. & Gosso G. (1983) - Assetto geologico strutturale della falda piemontese nel settore dell`alta valle di Viù (Alpi occidentali). Memorie Società Geologica Italiana, 26, 479–483.

Pleuger J., Roller S., Walter J.M., Jansen E. & Froitzheim N. (2007) - Structural evolution of the contact between two Penninic nappes (Zermatt-Saas zone and Combin zone, Western Alps) and implications for the exhumation mechanism and paleogeography. International Journal of Earth Sciences, 96, 229–252.

Poli S. & Schmidt M.W. (1998) - The high-pressure stability of zoisite and phase relationships of zoisite-bearing assemblages. Contribution to Mineralogy and Petrology, 130, 162–175.

Polino R., Dal Piaz G.V. & Gosso G. (1990) - Tectonic erosion at the Adria margin and accretionary processes for the Cretaceous orogeny of the Alps. Mémoires de la Société Géologique de France, 156, 345–367.

Powell R. & Holland T.J.B. (1988) - An internally consistent dataset with uncertainties and correlations: 3. Applications to geobarometry, worked examples and a computer program. Journal of Metamorphic Geology, 6, 173–204.

Raimbourg H. & Kimura G. (2008) - Non-lithostatic pressure in subduction zones. Earth and Planetary Science Letters, 274, 414–422.

Regis D. (2007) - La scaglia austroalpina di Etirol-Levaz (Valtournenche, Valle d'Aosta): nuovi dati sulla traiettoria metamorfica prograde e sul picco eclogitico. MSc Thesis, University of Torino (Italy), 98p.

Reinecke T. (1991) - Very-high-pressure metamorphism and uplift of coesite-bearing metasediments from the Zermatt-Saas zone western Alps. European Journal of Mineralogy, 3, 7–17.

Reinecke T. (1998) - Prograde high- to ultrahigh-pressure metamorphism and exhumation of oceanic sediments at Lago di Cignana, Zermatt-Saas zone, Western Alps. Lithos, 42, 147–190.

DOI: 10.3301/GFT.2014.01

Reinecke T., van der Klauw S.N.G.C. & Stöckhert B. (1994) - UHP metamorphic oceanic crust of the Zermatt-Saas zone (Piemontese zone) at Lago di Cignana, Valtournenche, Italy. In: R. Compagnoni, B. Messiga & D. Castelli (Eds.), High Pressure Metamorphism in the Western Alps, Guide-book to the field excursion B1, 16th General Meeting of the International Mineralogical Association, 10–15 September 1994, Pisa, Italy, 117–126. Ovidiografica, Pino Torinese.

Rubatto D., Gebauer D. & Fanning M. (1998) - Jurassic formation and Eocene subduction of the Zermatt–Saas–Fee ophiolites: implications for the geodynamic evolution of the Central and Western Alps. Contributions to Mineralogy and Petrology, 132, 269–287.

Saliot P. (1979) - La jadéite dans les Alpes françaises. Bull. Soc. Française. Min. Crist., 102, 391–401.

Schärer U., Cannic S. & Lapierre H. (2000) - Preliminary evidence for a Hercynian age of the Versoyen complex, Western Alps. Comptes Rendus de l'Académie des Sciences de Paris, 330, 325-332.

Schreyer W., Bernhardt H.-J. & Medenbach O. (1992) - Petrologic evidence for a rhodochrosite precursor of spessartine in coticules of the Venn-Stavelot Massif, Belgium. Mineralogical Magazine, 56, 527–532.

Schürch M.L. (1987) - Les ophiolites de la zone du Versoyen (France - Italie). Schweizerische mineralogische und petrographische Mitteilungen, 67, 374-375.

Skora S., Lapen T.J., Baumgartner L.P., Johnson C.M., Hellebrand E. & Mahlen N.J. (2009) - The duration of prograde garnet crystallization in the UHP eclogites at Lago di Cignana, Italy. Earth and Planetary Science Letters, 287, 402–411.

Sodero D. (1968) - Sull'età Barremiano-Aptiano delle formazioni basali del "Flysch" della Zona delle Brecce di Tarantasia in Valle d'Aosta. Bollettino Società Geologica Italiana, 87, 223-231.

Tamagno E. (2000) - L'unità meta-ofiolitica di pressione molto alta del Lago di Cignana (Valtournenche – Aosta) e le sue relazioni con le unità tettoniche vicine. Unpubl. M.Sc. Thesis, University of Torino (Italy), 188p.

Trümpy R. (1949) - Der Lias der Glarner Alpen. Denkschr. Schweiz. Nat. forsch. Ges., E.T.H. Zuerich, Switzerland, 79, 193 pp.

Trümpy R. (1951) - Remarques sur les racines helvétiques et les Schistes lustrés entre le Rhône et la Vallée de Bagnes (Région de la Pierre Avoi). Eclogae geologicae Helvetiae, 44, 338–442.

Trümpy R. (1980) - Geology of Switzerland: a guide book. Part A. An outline of the Geology of Switzerland, with contrubutions by D. Bernoulli, M. Grünenfelder, V. Köppel. St. Müller & V. Trommsdorff. Wepf and Co., Basel, 104 pp.

van der Klauw S.N.G.C., Reinecke T. & Stöckhert B. (1997) - Exhumation of ultrahigh-pressure metamorphic oceanic crust from Lago di Cignana, Piemontese zone, Western Alps: the structural record in metabasites. Lithos, 41, 79–102.

Vitale Brovarone A., Beltrando M., Malavieille J., Giuntoli F., Tondella E., Groppo C., Beyssac O. & Compagnoni R. (2011) - Inherited Ocean-Continent Transition zones in deeply subducted terranes: Insights from Alpine Corsica. Lithos, 124, 273-290, doi: 10.1016/j.lithos.2011.02.013

Vitale Brovarone A., Beyssac O., Malavieille J., Molli G., Beltrando M. & Compagnoni R. (2013) - Stacking of continuous segments of subducted lithosphere in high-pressure orogens: architecture of Alpine Corsica (France). Earth Science Reviews, 116, 35-56.

Yamato P., Agard P., Burov E., Le Pourhiet L., Jolivet L. & Tiberi C. (2007) - Burial and exhumation in a subduction wedge: Mutual constraints from thermomechanical modeling and natural P-T-t data (Schistes Lustrés, Western Alps). Journal of Geophysical Research Solid Earth, 112, 28 pp.; B07410, doi:10.1029/2006jb004441

DOI: 10.3301/GFT.2014.01